

Weak Pion and Photon Production off Nucleons in a Chiral Effective Field Theory

Brian D. Serot* and Xilin Zhang†

*Department of Physics and Center for Exploration of Energy and Matter
Indiana University, Bloomington, IN 47405*

(Dated: April 14, 2021)

Abstract

Neutrino-induced pion and photon production from nucleons and nuclei are important for the interpretation of neutrino-oscillation experiments, and these processes are potential backgrounds in the MiniBooNE experiment [A. A. Aquilar-Arevalo *et al.* (MiniBooNE Collaboration), Phys. Rev. Lett. **100**, 032301 (2008)]. Pion and photon production are investigated at intermediate energies, where the Δ resonance becomes important. The Lorentz-covariant effective field theory contains nucleons, pions, Deltas, isoscalar scalar (σ) and vector (ω) fields, and isovector vector (ρ) fields. The lagrangian exhibits a nonlinear realization of (approximate) $SU(2)_L \otimes SU(2)_R$ chiral symmetry and incorporates vector meson dominance. Power counting for vertices and Feynman diagrams involving the Δ is explained. Because of the built-in symmetries, the vector currents are automatically conserved, and the axial-vector currents satisfy PCAC. The irrelevance of so-called off-shell Δ couplings and the structure of the dressed Δ propagator, which has a pole only in the spin-3/2 channel, are discussed. To calibrate the axial-vector transition current ($N \leftrightarrow \Delta$), pion production from the nucleon is used as a benchmark and compared to bubble-chamber data from Argonne and Brookhaven National Laboratories. At low energies, the convergence of our power-counting scheme is investigated, and next-to-leading-order tree-level corrections are found to be very small.

PACS numbers: 12.15.Ji; 25.30.Pt; 11.30.Rd; 24.10.Jv; 14.20.Gk

*Electronic address: serot@indiana.edu

†Electronic address: xilzhang@indiana.edu

I. INTRODUCTION

Weak pion production from nucleons and nuclei plays an important role in the interpretation of neutrino-oscillation experiments, such as MiniBooNE [1] and K2K [2]. Pion absorption after production will lead to events that mimic quasielastic scattering. Moreover, neutral current (NC) π^0 and photon production produce detector signals that resemble those of the desired e^\pm signals. Finally, NC π^0 and photon production might explain the excess events seen at low energies in MiniBooNE.

Ultimately, the calculations must be done on nuclei, which are the primary detector materials in oscillation experiments. To separate the many-body effects from the reaction mechanism and to calibrate the elementary amplitude, we will study charged current (CC) and NC pion and photon production from free nucleons. We will apply our full lagrangian to the many-body problem in a forthcoming paper.

In this work, we use a recently proposed Lorentz-covariant meson–baryon effective field theory (EFT) that was originally motivated by the nuclear many-body problem [3–10]. (This formalism is often called *quantum hadrodynamics* or QHD.) This QHD EFT includes all the relevant symmetries of the underlying QCD; in particular, the approximate, spontaneously broken $SU(2)_L \otimes SU(2)_R$ chiral symmetry is realized nonlinearly. The motivation for this EFT and some calculated results are discussed in Refs. [4, 5, 11–20].

Here we consistently incorporate the $\Delta(1232)$ resonance as an explicit degree of freedom in this EFT, while respecting the underlying symmetries of QCD noted earlier. We are concerned with the intermediate-energy region ($E_\nu^{\text{Lab}} < 1 \text{ GeV}$), where the resonant behavior of the Δ is important. Couplings to electroweak fields are included using the external field procedure [21], which allows us to deduce the electroweak currents. Because of the approximate symmetries contained in the lagrangian, the vector currents are explicitly conserved, and the axial-vector currents satisfy PCAC. Form factors are generated within the theory by vector meson dominance (VMD), which avoids introducing phenomenological form factors and makes current conservation manifest. We discuss the power counting of both vertices and diagrams on and off resonance and consistently keep all tree-level diagrams through next-to-leading order.

The goal of this work is to use CC and NC pion production from nucleons to serve as a benchmark calculation. In a future paper, we will include the electroweak response of the nuclear many-body system to discuss pion production from nuclei.

There have been numerous earlier studies of weak pion production off nucleons in the energy regime where the Δ is important [22–33]. It is typically assumed that the vector part of the $N \rightarrow \Delta$ transition current is well constrained by electromagnetic interactions [29, 31]. The uncertainty is in the axial-vector part of the current, which is determined by fitting to ANL [34] and BNL [35] bubble-chamber data. The data has large error bars, which leads to significant model dependence in the fitted results [30, 32, 36]. In this work, we choose one recently fitted parametrization [32] and use it to determine the momentum dependence of the transition current vertices. We also use it to determine the constants of our VMD parametrization. We then compare calculations with both sets of vertices to the data at low and intermediate neutrino energies.

This paper is organized as follows: in Sec. II, we introduce our EFT lagrangian and calculate several current matrix elements that will be useful for the subsequent Feynman diagram calculations. The theory involving the Δ is emphasized, and the pathologies of introducing the Δ in quantum field theory are clarified, which is the basis of the lagrangian

construction. Then the transition current basis and form factors are discussed carefully. In Sec. III, we show the detailed calculations for CC and NC pion production and for the NC photon production cross sections. We initially insist on approaching this problem within EFT, and hence consider only the low-energy region: $E_\nu^{\text{Lab}} \leq 0.5 \text{ GeV}$. After that, we show our results in Sec. IV. Whenever possible, we compare our results with available data and present our analysis. Finally, our conclusions are summarized in Sec. V.

In the Appendixes, we discuss isospin conventions; C , P , and T properties of various fields; form factors; the Δ propagator; and kinematics.

II. FORMALISM

A. Notation

In this calculation, we use the metric $g_{\mu\nu} = \text{diag}(1, -1, -1, -1)_{\mu\nu}$, and the convention for the Levi-Civita symbol $\epsilon^{\mu\nu\alpha\beta}$ is $\epsilon^{0123} = 1$. The Dirac matrices are represented as (here σ^i is a Pauli matrix)

$$\gamma^0 = \begin{pmatrix} \mathbf{1} & 0 \\ 0 & -\mathbf{1} \end{pmatrix}, \quad \gamma^1 = \begin{pmatrix} 0 & \sigma^x \\ -\sigma^x & 0 \end{pmatrix}, \quad \gamma^2 = \begin{pmatrix} 0 & \sigma^y \\ -\sigma^y & 0 \end{pmatrix}, \quad \gamma^3 = \begin{pmatrix} 0 & \sigma^z \\ -\sigma^z & 0 \end{pmatrix}, \quad (1)$$

and $\gamma^5 = i\gamma^0\gamma^1\gamma^2\gamma^3$.

Since we are going to include the Δ , which is the lowest N resonance, and whose isospin is $I = 3/2$, we will define the conventions for isospin indices. We will work with spherical vector components for the pion field, which requires some care with signs. Begin with

$$\Delta^{*a} \equiv T_{iA}^a \Delta^{*iA}, \quad (2)$$

Here $a = \pm 3/2, \pm 1/2$, $i = \pm 1, 0$, and $A = \pm 1/2$. The upper components labeled ‘ a ’, ‘ i ’, and ‘ A ’ furnish $\mathcal{D}^{(3/2)}$, $\mathcal{D}^{(1)}$, and $\mathcal{D}^{(1/2)}$ representations of the isospin $SU(2)$ group. We can immediately see that $T_{iA}^a = \langle 1, \frac{1}{2}; i, A | \frac{3}{2}; a \rangle$, which are CG coefficients. It is well known that the conjugate representation of $SU(2)$ is equivalent to the representation itself, so we introduce a metric linking the two representations to raise or lower the indices a, i , and A . For example, $\Delta_a \equiv (\Delta^{*a})^* = T_a^{\dagger iA} \Delta_{iA}$, where $T_a^{\dagger iA} = \langle \frac{3}{2}; a | 1, \frac{1}{2}; i, A \rangle$, can be written as

$$\Delta_a = T_a^{iA} \Delta_{iA} \equiv T_{jB}^b \tilde{\delta}_{ba} \tilde{\delta}^{ji} \tilde{\delta}^{BA} \Delta_{iA}. \quad (3)$$

Here, $\tilde{\delta}$ denotes a metric for one of the three representations. So in this convention, $T_a^{\dagger iA} = T_a^{iA}$, which is straightforward to prove. Details about the conventions are given in Appendix A.

B. Lagrangian without $\Delta(1232)$

It is widely accepted that the approximate global chiral symmetry $SU(2)_L \otimes SU(2)_R \otimes U(1)_B$ in two-flavor QCD is spontaneously broken to $SU(2)_V \otimes U(1)_B$, while also being manifestly broken due to the small quark masses. To implement such broken global symmetry in the effective lagrangian using hadronic degrees of freedom, it was found that there exists a general nonlinear realization of such symmetry [37–39]. Sometime later, in Ref. [40], the

concept of phenomenological lagrangians was revisited, leading to the wide use of effective field theory, in which chiral symmetry is realized nonlinearly.

Here we will make use of the background field method to construct a low-energy effective field theory. In this method, we elevate the global symmetry $SU(2)_L \otimes SU(2)_R \otimes U(1)_B$ to a local symmetry [21, 41, 42].

First, we will only briefly discuss how the elevated local symmetry is realized in two-flavor QCD, since this material can be easily found elsewhere (see Ref. [42], for example), and then we show how this symmetry is realized nonlinearly in QHD. This theory is well developed in Refs. [4, 5, 10]. Since we take a different approach, we will detail the chiral symmetry realization in this section. Finally, we will talk about the electroweak interactions of hadrons.

1. Chiral symmetry realization

The charge algebra of $SU(2)_L \otimes SU(2)_R \otimes U(1)_B$ is (we will henceforth ignore the *tilde* on $\tilde{\delta}$ and $\tilde{\epsilon}$)

$$\begin{aligned}
[Q_L^i, Q_L^j] &= i\epsilon^{ijk} Q_{Lk} , \\
[Q_R^i, Q_R^j] &= i\epsilon^{ijk} Q_{Rk} , \\
[Q_L^i, Q_R^j] &= 0 , \\
[Q_B, Q_{L,R}^i] &= 0 , \quad \text{where } i, j, k = +1, 0, -1 .
\end{aligned} \tag{4}$$

We can immediately see that massless, two-flavor QCD has this symmetry, with background fields including $\mathbf{v}^\mu \equiv \mathbf{v}^{i\mu}\tau_i/2$ (isovector vector), $\mathbf{v}_{(s)}^\mu$ (isoscalar vector), $\mathbf{a}^\mu \equiv \mathbf{a}^{i\mu}\tau_i/2$ (isovector axial-vector), $\mathbf{s} \equiv \mathbf{s}^i\tau_i/2$ (isovector scalar), and $\mathbf{p} \equiv \mathbf{p}^i\tau_i/2$ (isovector pseudoscalar), where $i = x, y, z$ or $+1, 0, -1$:

$$\begin{aligned}
\mathcal{L} &= \mathcal{L}_{QCD} + \bar{q}\gamma_\mu(\mathbf{v}^\mu + B\mathbf{v}_{(s)}^\mu + \gamma_5\mathbf{a}^\mu)q - \bar{q}(\mathbf{s} - i\gamma_5\mathbf{p})q \\
&= \mathcal{L}_{QCD} + \bar{q}_L\gamma_\mu(l^\mu + B\mathbf{v}_{(s)}^\mu)q_L + \bar{q}_R\gamma_\mu(r^\mu + B\mathbf{v}_{(s)}^\mu)q_R \\
&\quad - \bar{q}_L(\mathbf{s} - i\mathbf{p})q_R - \bar{q}_R(\mathbf{s} + i\mathbf{p})q_L .
\end{aligned} \tag{5}$$

Here, $r^\mu = \mathbf{v}^\mu + \mathbf{a}^\mu$, $l^\mu = \mathbf{v}^\mu - \mathbf{a}^\mu$, $q_L = \frac{1}{2}(1 - \gamma^5)q$, $q_R = \frac{1}{2}(1 + \gamma^5)q$, and $B = 1/3$ is the baryon number. The symmetry transformation rules are

$$\begin{aligned}
q_{LA} &\rightarrow \exp\left[-i\frac{\theta(x)}{3}\right] \left(\exp\left[-i\theta_{Li}(x)\frac{\tau^i}{2}\right]\right)_A^B q_{LB} \equiv \exp\left[-i\frac{\theta(x)}{3}\right] (L)_A^B q_{LB} , \\
q_R &\rightarrow \exp\left[-i\frac{\theta(x)}{3}\right] \exp\left[-i\theta_{Ri}(x)\frac{\tau^i}{2}\right] q_R \equiv \exp\left[-i\frac{\theta(x)}{3}\right] Rq_R , \\
l^\mu &\rightarrow L l^\mu L^\dagger + iL \partial^\mu L^\dagger , \\
r^\mu &\rightarrow R r^\mu R^\dagger + iR \partial^\mu R^\dagger , \\
\mathbf{v}_{(s)}^\mu &\rightarrow \mathbf{v}_{(s)}^\mu - \partial^\mu \theta , \\
\mathbf{s} + i\mathbf{p} &\rightarrow R(\mathbf{s} + i\mathbf{p})L^\dagger , \quad \mathbf{s} - i\mathbf{p} \rightarrow L(\mathbf{s} - i\mathbf{p})R^\dagger .
\end{aligned} \tag{6}$$

We can also construct field strength tensors that transform homogeneously:

$$\begin{aligned}
f_{L\mu\nu} &\equiv \partial_\mu l_\nu - \partial_\nu l_\mu - i[l_\mu, l_\nu] \rightarrow L f_{L\mu\nu} L^\dagger, \\
f_{R\mu\nu} &\equiv \partial_\mu r_\nu - \partial_\nu r_\mu - i[r_\mu, r_\nu] \rightarrow R f_{R\mu\nu} R^\dagger, \\
f_{s\mu\nu} &\equiv \partial_\mu \mathbf{v}_{(s)\nu} - \partial_\nu \mathbf{v}_{(s)\mu} \rightarrow f_{s\mu\nu}.
\end{aligned} \tag{7}$$

Meanwhile, to conserve C , P , and T symmetry, we have the corresponding transformation rules shown in Appendix B.

Now we proceed to discuss low-energy nuclear theory involving π^i , ρ_μ^i , N^A , and the chiral singlets V_μ and ϕ [5]. As noted earlier, chiral symmetry is spontaneously broken at low energy in the chiral limit, and the symmetry is realized nonlinearly:

$$\begin{aligned}
U &\equiv \exp \left[2i \frac{\pi_i(x)}{f_\pi} t^i \right] \rightarrow L U R^\dagger, \\
\xi &\equiv \sqrt{U} = \exp \left[i \frac{\pi_i}{f_\pi} t^i \right] \rightarrow L \xi h^\dagger = h \xi R^\dagger, \\
\tilde{v}_\mu &\equiv \frac{-i}{2} [\xi^\dagger (\partial_\mu - i l_\mu) \xi + \xi (\partial_\mu - i r_\mu) \xi^\dagger] \equiv \tilde{v}_{i\mu} t^i \rightarrow h \tilde{v}_\mu h^\dagger - i h \partial_\mu h^\dagger, \\
\tilde{a}_\mu &\equiv \frac{-i}{2} [\xi^\dagger (\partial_\mu - i l_\mu) \xi - \xi (\partial_\mu - i r_\mu) \xi^\dagger] \equiv \tilde{a}_{i\mu} t^i \rightarrow h \tilde{a}_\mu h^\dagger, \\
\tilde{\partial}_\mu U &\equiv \partial_\mu U - i l_\mu U + i U r_\mu \rightarrow L \tilde{\partial}_\mu U R^\dagger, \\
(\tilde{\partial}_\mu \psi)_\alpha &\equiv (\partial_\mu + i \tilde{v}_\mu - i \mathbf{v}_{(s)\mu} B)_\alpha^\beta \psi_\beta \rightarrow \exp[-i\theta(x)B] h_\alpha^\beta (\tilde{\partial}_\mu \psi)_\beta, \\
\tilde{v}_{\mu\nu} &\equiv -i[\tilde{a}_\mu, \tilde{a}_\nu] \rightarrow h \tilde{v}_{\mu\nu} h^\dagger, \\
F_{\mu\nu}^{(+)} &\equiv \xi^\dagger f_{L\mu\nu} \xi + \xi f_{R\mu\nu} \xi^\dagger \rightarrow h F_{\mu\nu}^{(+)} h^\dagger, \\
F_{\mu\nu}^{(-)} &\equiv \xi^\dagger f_{L\mu\nu} \xi - \xi f_{R\mu\nu} \xi^\dagger \rightarrow h F_{\mu\nu}^{(-)} h^\dagger, \\
\tilde{\partial}_\lambda F_{\mu\nu}^{(\pm)} &\equiv \partial_\lambda F_{\mu\nu}^{(\pm)} + i[\tilde{v}_\lambda, F_{\mu\nu}^{(\pm)}] \rightarrow h \tilde{\partial}_\lambda F_{\mu\nu}^{(\pm)} h^\dagger.
\end{aligned} \tag{8}$$

In the preceding equations, t^i are the generators of reducible representations of $SU(2)$. Specifically, they could be generators of $\mathcal{D}_N^{(1/2)} \oplus \mathcal{D}_\rho^{(1)} \oplus \mathcal{D}_\Delta^{(3/2)}$, which operate on non-Goldstone isospin multiplets including the nucleon, ρ meson, and Δ . We will generically label these fields by $\psi_\alpha = (N_A, \rho_i, \Delta_a)_\alpha$. Most of the time, the choice of t^i is clear from the context. B is the baryon number of the particle. The transformations of the isospin and chiral singlets V_μ and ϕ are trivial. We will also make use of the dual field tensors, for example, $\overline{F}^{(\pm)\mu\nu} \equiv \epsilon^{\mu\nu\alpha\beta} F_{\alpha\beta}^{(\pm)}$, which have the same chiral transformations as the ordinary field tensors. Here we do not include the background fields \mathbf{s} and \mathbf{p} mentioned in Eq. (5), which are the source of manifest chiral-symmetry breaking in the Standard Model.

The realizations of C , P , and T symmetries are given in Appendix C.

2. Power counting and the lagrangian

Based on the transformation rules of the building blocks listed above, we can begin to construct the low-energy EFT lagrangian. The organization of interaction terms in this

lagrangian is based on power counting [5]. The power counting in EFT essentially assumes that when the interaction structure becomes more complicated, i.e., more fields and more derivatives are introduced, its contribution to physical observables becomes less important. Similarly, loop contributions will be suppressed more when the number of loops gets bigger. The validity of this assumption is connected with Naive Dimensional Analysis (NDA) [43, 44] which assumes the strength (coupling) of the interaction is of order unity when the appropriate dimensional scale factors have been included. This “naturalness” can be checked only after the calculations are finished.

To make the power counting transparent, we can associate with each interaction term an index

$$\hat{\nu} \equiv d + \frac{n}{2} + b . \quad (9)$$

Here d is the number of derivatives (small momentum transfer) in the interaction, n is the number of fermion fields, and b is the number of heavy meson fields. Since the lagrangian is well developed in Refs. [10, 45], we just outline the lagrangian here. We begin with

$$\begin{aligned} \mathcal{L}_{N(\hat{\nu} \leq 3)} = & \bar{N}(i\gamma^\mu[\tilde{\partial}_\mu + ig_\rho\rho_\mu + ig_v V_\mu] + g_A\gamma^\mu\gamma^5\tilde{a}_\mu - M + g_s\phi)N \\ & - \frac{f_\rho g_\rho}{4M}\bar{N}\rho_{\mu\nu}\sigma^{\mu\nu}N - \frac{f_v g_v}{4M}\bar{N}V_{\mu\nu}\sigma^{\mu\nu}N - \frac{\kappa_\pi}{M}\bar{N}\tilde{v}_{\mu\nu}\sigma^{\mu\nu}N \\ & + \frac{4\beta_\pi}{M}\bar{N}N\text{Tr}(\tilde{a}_\mu\tilde{a}^\mu) + \frac{i\kappa_1}{2M^2}\bar{N}\gamma_\mu\overset{\leftrightarrow}{\partial}_\nu N\text{Tr}(\tilde{a}^\mu\tilde{a}^\nu) \\ & + \frac{1}{4M}\bar{N}\sigma^{\mu\nu}(2\lambda^{(0)}f_{s\mu\nu} + \lambda^{(1)}F_{\mu\nu}^{(+)}N) , \end{aligned} \quad (10)$$

where $\tilde{\partial}_\mu$ is defined in Eq. (8), $\tilde{\partial}_\nu \equiv \partial_\nu - (\overset{\leftarrow}{\partial}_\nu - i\tilde{v}_\nu + i\mathbf{v}_{(s)\nu})$, and the new field tensors are $V_{\mu\nu} \equiv \partial_\mu V_\nu - \partial_\nu V_\mu$ and

$$\rho_{\mu\nu} \equiv \partial_{[\mu}\rho_{\nu]} + i\bar{g}_\rho[\rho_\mu, \rho_\nu] + i([\tilde{v}_\mu, \rho_\nu] - \mu \leftrightarrow \nu) \rightarrow h\rho_{\mu\nu}h^\dagger . \quad (11)$$

The superscripts ⁽⁰⁾ and ⁽¹⁾ denote the isospin.

Next is a purely mesonic term:

$$\begin{aligned} \mathcal{L}_{\text{meson}(\hat{\nu} \leq 4)} = & \frac{1}{2}\partial_\mu\phi\partial^\mu\phi + \frac{1}{4}f_\pi^2\text{Tr}[\tilde{\partial}_\mu U(\tilde{\partial}^\mu U)^\dagger] + \frac{1}{4}f_\pi^2 m_\pi^2\text{Tr}(U + U^\dagger - 2) \\ & - \frac{1}{2}\text{Tr}(\rho_{\mu\nu}\rho^{\mu\nu}) - \frac{1}{4}V^{\mu\nu}V_{\mu\nu} \\ & + \frac{1}{2}\left(1 + \eta_1\frac{g_s\phi}{M} + \frac{\eta_2 g_s^2\phi^2}{2M^2}\right)m_v^2 V_\mu V^\mu + \frac{1}{4!}\zeta_0 g_v^2(V_\mu V^\mu)^2 \\ & + \left(1 + \eta_\rho\frac{g_s\phi}{M}\right)m_\rho^2\text{Tr}(\rho_\mu\rho^\mu) - \left(\frac{1}{2} + \frac{\kappa_3 g_s\phi}{3!M} + \frac{\kappa_4 g_s^2\phi^2}{4!M^2}\right)m_s^2\phi^2 \\ & + \frac{1}{2g_\gamma}\left(\text{Tr}(F^{(+)\mu\nu}\rho_{\mu\nu}) + \frac{1}{3}f_s^{\mu\nu}V_{\mu\nu}\right) . \end{aligned} \quad (12)$$

The $\nu = 3$ and $\nu = 4$ terms in $\mathcal{L}_{\text{meson}(\hat{\nu} \leq 4)}$ are important for describing the bulk properties of nuclear many-body systems [5, 46, 47]. The only manifest chiral-symmetry breaking is through the nonzero pion mass.

Finally, we have

$$\begin{aligned}
\mathcal{L}_{N,\pi(\hat{\nu}=4)} &= \frac{1}{2M^2} \bar{N} \gamma_\mu (2\beta^{(0)} \partial_\nu f_s^{\mu\nu} + \beta^{(1)} \tilde{\partial}_\nu F^{(+)\mu\nu} + \beta_A^{(1)} \gamma^5 \tilde{\partial}_\nu F^{(-)\mu\nu}) N \\
&\quad - \omega_1 \text{Tr}(F_{\mu\nu}^{(+)} \tilde{v}^{\mu\nu}) + \omega_2 \text{Tr}(\tilde{a}_\mu \tilde{\partial}_\nu F^{(-)\mu\nu}) + \omega_3 \text{Tr}(\tilde{a}_\mu i [\tilde{a}_\nu, F^{(+)\mu\nu}]) \\
&\quad - g_{\rho\pi\pi} \frac{2f_\pi^2}{m_\rho^2} \text{Tr}(\rho_{\mu\nu} \tilde{v}^{\mu\nu}) \\
&\quad + \frac{c_1}{M^2} \bar{N} \gamma^\mu N \text{Tr}(\tilde{a}^\nu \bar{F}_{\mu\nu}^{(+)}) + \frac{e_1}{M^2} \bar{N} \gamma^\mu \tilde{a}^\nu N \bar{f}_{s\mu\nu} \\
&\quad + \frac{c_{1\rho} g_\rho}{M^2} \bar{N} \gamma^\mu N \text{Tr}(\tilde{a}^\nu \bar{\rho}_{\mu\nu}) + \frac{e_{1\nu} g_\nu}{M^2} \bar{N} \gamma^\mu \tilde{a}^\nu N \bar{V}_{\mu\nu} .
\end{aligned} \tag{13}$$

Note that $\mathcal{L}_{N,\pi(\hat{\nu}=4)}$ is not a complete list of all possible $\hat{\nu} = 4$ interaction terms. However, $\beta^{(0)}$ and $\beta^{(1)}$ will be used in the form factors of the nucleon's vector current, $\omega_{1,2,3}$ will contribute to the form factor of the pion's vector current, and $g_{\rho\pi\pi}$ will be used in the form factors that incorporate vector meson dominance. The constants $c_1, e_1, c_{1\rho}$, and $e_{1\rho}$ will be explained later when we discuss photon production.

3. Contributions to current matrix elements from irreducible diagrams

By comparing Eq. (5) with the electroweak interactions of quarks in the Standard Model [48, 49], we can determine the form of the background fields in terms of the vector bosons W_μ^\pm, Z_μ , and A_μ :

$$\begin{aligned}
l_\mu &= -e \frac{\tau^0}{2} A_\mu + \frac{g}{\cos \theta_w} \sin^2 \theta_w \frac{\tau^0}{2} Z_\mu \\
&\quad - \frac{g}{\cos \theta_w} \frac{\tau^0}{2} Z_\mu - gV_{ud} \left(W_\mu^{+1} \frac{\tau_{+1}}{2} + W_\mu^{-1} \frac{\tau_{-1}}{2} \right) ,
\end{aligned} \tag{14}$$

$$r_\mu = -e \frac{\tau^0}{2} A_\mu + \frac{g}{\cos \theta_w} \sin^2 \theta_w \frac{\tau^0}{2} Z_\mu , \tag{15}$$

$$v_{(s)\mu} = -e \frac{1}{2} A_\mu + \frac{g}{\cos \theta_w} \sin^2 \theta_w \frac{1}{2} Z_\mu , \tag{16}$$

where g is the $SU(2)$ charge, and θ_w is the weak mixing angle. Furthermore:

$$\begin{aligned}
f_{L\mu\nu} &= -e \frac{\tau^0}{2} A_{[\nu,\mu]} + \frac{g}{\cos \theta_w} \sin^2 \theta_w \frac{\tau^0}{2} Z_{[\nu,\mu]} - \frac{g}{\cos \theta_w} \frac{\tau^0}{2} Z_{[\nu,\mu]} \\
&\quad - gV_{ud} \frac{\tau^{+1}}{2} W_{+1[\nu,\mu]} - gV_{ud} \frac{\tau^{-1}}{2} W_{-1[\nu,\mu]} \\
&\quad + \text{interference terms including } (WZ), (WA), (WW), \text{ but no } (ZA) ,
\end{aligned} \tag{17}$$

$$f_{R\mu\nu} = -e \frac{\tau^0}{2} A_{[\nu,\mu]} + \frac{g}{\cos \theta_w} \sin^2 \theta_w \frac{\tau^0}{2} Z_{[\nu,\mu]} \quad (\text{no interference terms}) , \tag{18}$$

$$f_{s\mu\nu} = -e \frac{1}{2} A_{[\nu,\mu]} + \frac{g}{\cos \theta_w} \sin^2 \theta_w \frac{1}{2} Z_{[\nu,\mu]} . \tag{19}$$

If we define [see Eq. (5)]

$$\begin{aligned}\mathcal{L}_{\text{ext}} &\equiv \mathbf{v}_{i\mu} V^{i\mu} - \mathbf{a}_{i\mu} A^{i\mu} + \mathbf{v}_{(s)\mu} J^{B\mu} \\ &= J_{i\mu}^L l^{i\mu} + J_{i\mu}^R r^{i\mu} + \mathbf{v}_{(s)\mu} J^{B\mu} ,\end{aligned}\quad (20)$$

$$\mathcal{L}_I = -e J_{\mu}^{EM} A^{\mu} - \frac{g}{\cos\theta_w} J_{\mu}^{NC} Z^{\mu} - g V_{ud} J_{+1\mu}^L W^{+1\mu} - g V_{ud} J_{-1\mu}^L W^{-1\mu} , \quad (21)$$

and use Eqs. (14) to (16), we can easily discover

$$J_{i\mu}^L \equiv \frac{1}{2} (V_{i\mu} + A_{i\mu}) , \quad (22)$$

$$J_{i\mu}^R \equiv \frac{1}{2} (V_{i\mu} - A_{i\mu}) , \quad (23)$$

$$J_{\mu}^{EM} = V_{\mu}^0 + \frac{1}{2} J_{\mu}^B , \quad (24)$$

$$J_{\mu}^{NC} = J_{\mu}^{L0} - \sin^2\theta_w J_{\mu}^{EM} . \quad (25)$$

Here, J_{μ}^B is the baryon current, defined to be coupled to $\mathbf{v}_{(s)}^{\mu}$. These relations are consistent with the charge algebra $Q = T^0 + B/2$. (B is the baryon number.) $V^{i\mu}$ and $A^{i\mu}$ are the isovector vector current and the isovector axial-vector current, respectively. We do not discuss ‘‘seagull’’ terms of higher order in the couplings because they do not enter in our calculations [10, 50].

Based on the equations given above and the EFT lagrangian, we can calculate the matrix elements $\langle N | V_{\mu}^i, A_{\mu}^i, J_{\mu}^B | N \rangle$ and $\langle N; \pi | V_{\mu}^i, A_{\mu}^i, J_{\mu}^B | N \rangle$ at tree level; loops are not included.¹ Since non-Goldstone vector bosons are included here, then by vector meson dominance (VMD), we can extrapolate the current away from $Q^2 = 0$ to some extent [10, 20]. The results are given below, and the explicit calculations are shown in Appendix D. Note that q^{μ} is defined as the *incoming* momentum transfer at the vertex; in terms of initial and final nucleon momenta, $q^{\mu} \equiv p_{n_f}^{\mu} - p_{n_i}^{\mu}$. Similarly, $q^{\mu} + p_{n_i}^{\mu} = p_{n_f}^{\mu} + k_{\pi}^{\mu}$ for pion production.

$$\langle N, B | V_{\mu}^i | N, A \rangle = \langle B | \frac{\tau^i}{2} | A \rangle \bar{u}_f \left(\gamma_{\mu} + 2\delta F_1^{V,md} \frac{q^2 \gamma_{\mu} - \not{q} q_{\mu}}{q^2} + 2F_2^{V,md} \frac{\sigma_{\mu\nu} i q^{\nu}}{2M} \right) u_i \quad (26)$$

$$\equiv \langle B | \frac{\tau^i}{2} | A \rangle \bar{u}_f \Gamma_{V\mu}(q) u_i \quad (27)$$

$$\stackrel{\text{on shell}}{\equiv} \langle B | \frac{\tau^i}{2} | A \rangle \bar{u}_f \left(2F_1^{V,md} \gamma_{\mu} + 2F_2^{V,md} \frac{\sigma_{\mu\nu} i q^{\nu}}{2M} \right) u_i , \quad (28)$$

¹ The expressions for the currents listed below differ from those in Refs. [10, 51] because contributions from non-minimal and vector meson dominance terms are included here.

$$\langle N, B | J_\mu^B | N, A \rangle = \delta_B^A \bar{u}_f \left(\gamma_\mu + 2\delta F_1^{S,md} \frac{q^2 \gamma_\mu - \not{q} q_\mu}{q^2} + 2F_2^{S,md} \frac{\sigma_{\mu\nu} i q^\nu}{2M} \right) u_i \quad (29)$$

$$\equiv \delta_B^A \bar{u}_f \Gamma_{B\mu}(q) u_i \quad (30)$$

$$\stackrel{\text{on shell}}{\equiv} \delta_B^A \bar{u}_f \left(2F_1^{S,md} \gamma_\mu + 2F_2^{S,md} \frac{\sigma_{\mu\nu} i q^\nu}{2M} \right) u_i, \quad (31)$$

$$\begin{aligned} \langle N, B; \pi, j, k_\pi | A_\mu^i | N, A \rangle &= -\frac{\epsilon_{jk}^i}{f_\pi} \langle B | \frac{\tau^k}{2} | A \rangle \bar{u}_f \gamma^\nu u_i \\ &\times \left[g_{\mu\nu} + 2\delta F_1^{V,md} ((q - k_\pi)^2) \frac{q \cdot (q - k_\pi) g_{\mu\nu} - (q - k_\pi)_\mu q_\nu}{(q - k_\pi)^2} \right] \\ &- \frac{\epsilon_{jk}^i}{f_\pi} \langle B | \frac{\tau^k}{2} | A \rangle \bar{u}_f \frac{\sigma_{\mu\nu} i q^\nu}{2M} u_i \left[2\lambda^{(1)} \right. \\ &\quad \left. + 2\delta F_2^{V,md} ((q - k_\pi)^2) \frac{q \cdot (q - k_\pi)}{(q - k_\pi)^2} \right] \end{aligned} \quad (32)$$

$$\equiv \frac{\epsilon_{jk}^i}{f_\pi} \langle B | \frac{\tau^k}{2} | A \rangle \bar{u}_f \Gamma_{A\pi\mu}(q, k_\pi) u_i. \quad (33)$$

Here ($m_\rho = 0.776$ GeV, $m_v = 0.783$ GeV):

$$F_1^{V,md} = \frac{1}{2} \left(1 + \frac{\beta^{(1)}}{M^2} q^2 - \frac{g_\rho}{g_\gamma} \frac{q^2}{q^2 - m_\rho^2} \right), \quad \beta^{(1)} = -1.35, \quad \frac{g_\rho}{g_\gamma} = 2.48, \quad (34)$$

$$F_2^{V,md} = \frac{1}{2} \left(2\lambda^{(1)} - \frac{f_\rho g_\rho}{g_\gamma} \frac{q^2}{q^2 - m_\rho^2} \right), \quad \lambda^{(1)} = 1.85, \quad f_\rho = 3.04, \quad (35)$$

$$F_1^{S,md} = \frac{1}{2} \left(1 + \frac{\beta^{(0)}}{M^2} q^2 - \frac{2g_v}{3g_\gamma} \frac{q^2}{q^2 - m_v^2} \right), \quad \beta^{(0)} = -1.40, \quad \frac{g_v}{g_\gamma} = 3.95, \quad (36)$$

$$F_2^{S,md} = \frac{1}{2} \left(2\lambda^{(0)} - \frac{2f_v g_v}{3g_\gamma} \frac{q^2}{q^2 - m_v^2} \right), \quad \lambda^{(0)} = -0.06, \quad f_v = -0.19, \quad (37)$$

$$\delta F_1^{V/S,md}(q^2) \equiv F_1^{V/S,md}(q^2) - F_1^{V/S,md}(0), \quad (38)$$

$$\delta F_2^{V/S,md}(q^2) \equiv F_2^{V/S,md}(q^2) - F_2^{V/S,md}(0). \quad (39)$$

If we follow a procedure similar to that used in calculating $\langle N | V_\mu^i | N \rangle$ and $\langle N; \pi | A_\mu^i | N \rangle$, we can expand the axial-vector current in powers of q^2 using the lagrangian constants g_A and $\beta_A^{(1)}$. In fact, we can improve on this by including the axial-vector meson ($a_{1\mu}$) contribution to the matrix elements, which would arise from the interactions: $g_{a_1} \bar{N} \gamma^\mu \gamma^5 a_{1\mu} N$ and $c_{a_1} \text{Tr} (F^{(-)\mu\nu} a_{1\mu\nu})$. Here $a_{1\mu} = a_{1i\mu} \tau^i / 2$ and $a_{1\mu\nu} \equiv \tilde{\partial}_\mu a_{1\nu} - \tilde{\partial}_\nu a_{1\mu}$, where $a_{1i\mu}$ are the fields of the a_1 meson (whose mass is denoted as $m_{a_1} = 1.26$ GeV). Then we obtain (details can

be found in Appendix D)

$$\begin{aligned}\langle N, B|A_\mu^i|N, A\rangle &= -G_A^{md}(q^2)\langle B|\frac{\tau^i}{2}|A\rangle\bar{u}_f\left(\gamma_\mu - \frac{q_\mu\not{q}}{q^2 - m_\pi^2}\right)\gamma^5 u_i \\ &\equiv \langle B|\frac{\tau^i}{2}|A\rangle\bar{u}_f\Gamma_{A\mu}(q)u_i,\end{aligned}\quad (40)$$

$$\begin{aligned}\langle N, B, \pi, j|V_\mu^i|N, A\rangle &= \frac{\epsilon_{jk}^i}{f_\pi}\langle B|\frac{\tau^k}{2}|A\rangle\bar{u}_f\left(G_A^{md}(0)\gamma_\mu\gamma^5\right. \\ &\quad \left. + \delta G_A^{md}((q - k_\pi)^2)\frac{q \cdot (q - k_\pi)g_{\mu\nu} - (q - k_\pi)_\mu q_\nu}{(q - k_\pi)^2}\gamma^\nu\gamma^5\right)u_i,\end{aligned}\quad (41)$$

$$\equiv \frac{\epsilon_{jk}^i}{f_\pi}\langle B|\frac{\tau^k}{2}|A\rangle\bar{u}_f\Gamma_{V\pi\mu}(q, k_\pi)u_i.\quad (42)$$

Here, the definitions of $G_A^{md}(q^2)$ and $\delta G_A^{md}(q^2)$ are

$$\begin{aligned}G_A^{md}(q^2) &\equiv g_A - \beta_A^{(1)}\frac{q^2}{M^2} - \frac{2c_{a_1}g_{a_1}q^2}{q^2 - m_{a_1}^2}, \\ g_A &= 1.26, \beta_A^{(1)} = 2.27, c_{a_1}g_{a_1} = 3.85,\end{aligned}\quad (43)$$

$$\delta G_A^{md}(q^2) \equiv G_A^{md}(q^2) - G_A^{md}(0) = G_A^{md}(q^2) - g_A.\quad (44)$$

For the pion's vector current form factor [5]:

$$\begin{aligned}\langle \pi, k, k_\pi|V_\mu^i|\pi, j, k_\pi - q\rangle &= i\epsilon_{kj}^i(2k_\pi - q)_\mu\left(1 - \frac{g_{\rho\pi\pi}}{g_\gamma}\frac{q^2}{q^2 - m_\rho^2}\right)\quad \text{pion on shell} \\ &\equiv i\epsilon_{kj}^i(2k_\pi - q)_\mu F_\pi^{md}(q^2), \quad \frac{g_{\rho\pi\pi}}{g_\gamma} = 1.20\end{aligned}\quad (45)$$

\implies (pion off shell)

$$\begin{aligned}\langle \pi, k, k_\pi|V_\mu^i|\pi, j, k_\pi - q\rangle &= i\epsilon_{kj}^i\left[(2k_\pi - q)_\mu + 2\delta F_\pi^{md}(q^2)\left(k_{\pi\mu} - \frac{q \cdot k_\pi}{q^2}q_\mu\right)\right] \\ &\equiv i\epsilon_{kj}^i P_{V\mu}(q, k_\pi),\end{aligned}\quad (46)$$

$$\text{with } \delta F_\pi^{md}(q^2) = F_\pi^{md}(q^2) - F_\pi^{md}(0).\quad (47)$$

To determine the couplings in Eqs. (34), (35), (36), (37), (43) and (45), we compare our results with the conventional experimentally fitted form factors [5, 52]. We make the behavior of the form factors near $q^2 = 0$ as close to the conventional form factors as possible. In this calculation, we fit our ‘md’ form factors to those in [52] for the nucleon’s vector and baryon current. The conventional nucleon’s axial-vector current used to fit our G_A^{md} is parameterized in literature [53] as $G_A(q^2) = g_A/(1 - q^2/M_A^2)^2$, with $g_A = 1.26$ and $M_A = 1.05$ GeV. As shown in Ref. [20], the form factors due to vector meson dominance become inadequate at $Q^2 \approx 0.3$ GeV². This is also true of the axial parametrization. This indicates that the EFT lagrangian is only applicable for $E_l \leq 0.5$ GeV in lepton–nucleon interactions, above which Q^2 exceeds the limit. This will be clarified in the kinematical analysis of Sec. IV A.

C. Lagrangian involving $\Delta(1232)$

1. Chiral symmetry and power counting

The Δ^{*a} belong to an $I = 3/2$ multiplet as non-Goldstone particles in the low-energy theory. The chiral symmetry realization involving non-Goldstone particles, $\psi_\alpha = (N_A, \rho_i, \Delta_a)_\alpha$, has been given generally in Sec. IIB 1. Moreover, in the power counting of vertices, the Δ is counted the same way as the nucleon.

2. Spin-3/2 particles as manifest degrees of freedom in field theory [54]

We briefly discuss the well-known pathologies of high-spin particles in field theory [55–59]. It was discovered that with strong couplings, or strong fields, or large field variations, a field theory involving high-spin fields cannot be self-consistent. These investigations were carried out in the lagrangian formalism with a finite number of interaction terms. The reason for the pathology is that the unphysical degrees of freedom of the Δ may contribute when the constraints on the Δ fields are lost after adding interactions. However, it has more recently been realized that the number of degrees of freedom is correct in low-energy effective field theory, which has, in principle, an infinite number of interaction terms, as long as we work in the limit of low-energy and weak (boson) fields [60–62]. As we know, in the low-energy effective field theory, the interactions and boson fields are scaled by $1/M \approx 1/(1 \text{ GeV})$. The essence of the argument is that in the perturbative picture, the spin-1/2 components of the off-shell Δ (treating the Δ as a stable particle) will behave as *local contact interactions* without pole structure, which should be calibrated together with the complete set of contact terms in the effective lagrangian.

Another issue is about the so-called off-shell couplings, which have the form $\gamma_\mu \psi^\mu$, $\partial_\mu \psi^\mu$, $\bar{\psi}^\mu \gamma_\mu$, and $\partial_\mu \bar{\psi}^\mu$, and which had also been discussed together with pathologies. From the modern effective field theory viewpoint, it has been concluded [63, 64] that these off-shell couplings are redundant. The physical picture of this will be clarified after introducing the lagrangian in Sec. IIC 3.

3. Lagrangian and Δ propagator renormalization

Consider first $\mathcal{L}_{\Delta; \pi, \rho, V, \phi}$ ($\hat{v} \leq 3$), which is essentially a copy of the corresponding lagrangian for nucleons:

$$\begin{aligned} \mathcal{L}_{\Delta; \pi, \rho, V, \phi} = & \frac{-i}{2} \bar{\Delta}_\mu^a \{ \sigma^{\mu\nu}, (i \tilde{\partial} - h_\rho \not{\rho} - h_v \not{V} - m + h_s \phi) \}_a^b \Delta_{b\nu} + \tilde{h}_A \bar{\Delta}_\mu^a \tilde{g}_a^b \gamma^5 \Delta_b^\mu \\ & - \frac{\tilde{f}_\rho h_\rho}{4m} \bar{\Delta}_\lambda \rho_{\mu\nu} \sigma^{\mu\nu} \Delta^\lambda - \frac{\tilde{f}_v h_v}{4m} \bar{\Delta}_\lambda V_{\mu\nu} \sigma^{\mu\nu} \Delta^\lambda \\ & - \frac{\tilde{\kappa}_\pi}{m} \bar{\Delta}_\lambda \tilde{v}_{\mu\nu} \sigma^{\mu\nu} \Delta^\lambda + \frac{4\tilde{\beta}_\pi}{m} \bar{\Delta}_\lambda \Delta^\lambda \text{Tr}(\tilde{a}^\mu \tilde{a}_\mu). \end{aligned} \quad (48)$$

Here the sub- and superscripts $a, b = (\pm 3/2, \pm 1/2)$, so the isovector mesons use the isospin-3/2 representation. A few words on pathologies and off-shell couplings are in order. Based

on $\mathcal{L}_{\Delta;\pi,\rho,V,\phi}$, we can find the free propagator for the Δ . Details are shown in Appendix E, and here we ignore $\mu\nu$ indices and isospin indices:

$$\begin{aligned}
S_F^0(p) &\equiv S_F^{0(\frac{3}{2})}(p) + S_F^{0(\frac{3}{2}\perp)}(p) \\
&= P^{(\frac{3}{2})} \frac{-1}{\not{p} - m + i\epsilon} P^{(\frac{3}{2})} \\
&\quad + P^{(\frac{3}{2}\perp)} \left[-\frac{1}{\sqrt{3}m} P_{12}^{(\frac{1}{2})} - \frac{1}{\sqrt{3}m} P_{21}^{(\frac{1}{2})} + P_{22}^{(\frac{1}{2})} \frac{2}{3m^2} (\not{p} + m) P_{22}^{(\frac{1}{2})} \right] P^{(\frac{3}{2}\perp)}. \quad (49)
\end{aligned}$$

The operator $P^{(\frac{3}{2})}$ projects the general Rarita–Schwinger field ψ_μ to spin-3/2 objects, while $P^{(\frac{3}{2}\perp)} \equiv \mathbf{1} - P^{(\frac{3}{2})}$ is the orthogonal projection operator. In Appendix E, we also show that the self-energy $\Sigma_{\mu\nu} = \Sigma^\Delta g_{\mu\nu} + \delta\Sigma_{\mu\nu}$ can be written as

$$\begin{aligned}
\Sigma &= P^{(\frac{3}{2})} \Sigma^\Delta P^{(\frac{3}{2})} + P^{(\frac{3}{2}\perp)} \Sigma P^{(\frac{3}{2}\perp)} \\
&\equiv \Sigma^{(\frac{3}{2})} + \Sigma^{(\frac{3}{2}\perp)}. \quad (50)
\end{aligned}$$

We can then renormalize the Δ propagator as follows:

$$\begin{aligned}
S_F &= (S_F^{0(\frac{3}{2})} + S_F^{0(\frac{3}{2}\perp)}) + (S_F^{0(\frac{3}{2})} + S_F^{0(\frac{3}{2}\perp)}) (\Sigma^{(\frac{3}{2})} + \Sigma^{(\frac{3}{2}\perp)}) (S_F^{0(\frac{3}{2})} + S_F^{0(\frac{3}{2}\perp)}) + \dots \\
&= S_F^{0(\frac{3}{2})} + S_F^{0(\frac{3}{2})} \Sigma^{(\frac{3}{2})} S_F^{0(\frac{3}{2})} + \dots \\
&\quad + S_F^{0(\frac{3}{2}\perp)} + S_F^{0(\frac{3}{2}\perp)} \Sigma^{(\frac{3}{2}\perp)} S_F^{0(\frac{3}{2}\perp)} + \dots \quad (51)
\end{aligned}$$

From this we can conclude that the renormalized propagator $S_F \equiv S_F^{(\frac{3}{2})} + S_F^{(\frac{3}{2}\perp)}$. The resonant contribution is $S_F^{(\frac{3}{2})} = S_F^{0(\frac{3}{2})} + S_F^{0(\frac{3}{2})} \Sigma^{(\frac{3}{2})} S_F^{0(\frac{3}{2})}$. The background contribution is $S_F^{(\frac{3}{2}\perp)} = S_F^{0(\frac{3}{2}\perp)} + S_F^{0(\frac{3}{2}\perp)} \Sigma^{(\frac{3}{2}\perp)} S_F^{0(\frac{3}{2}\perp)}$. We can see that renormalization will shift the pole position of the resonant part. Moreover, as long as power counting is valid, i.e., $O(\Sigma/M) \ll 1$, we will always be far away from the unphysical pole in the renormalized non-resonant part proportional to $\{1/[1 - O(\Sigma/M)]\}^{-1}$. This also suggests that we will not see an unphysical pole in the renormalized propagator, when we work in the low-energy perturbative region, where power counting makes sense. So we indeed have the right degrees of freedom in our low-energy theory, namely, a single pole at the resonance. Thus perturbative unitarity is not obviously violated in this theory with high-spin fields.

Another issue is the $1/p^2$ singularity in the projection operators. In principle, when we are in the low-energy region, $p^2 = (p_{ni} + k)^2$ is always positive (timelike) in all the channels. Here k is some general small momentum compared to p_{ni} , which is the nucleon's momentum that is almost on shell.

The preceding discussion also helps to clarify the redundancy of the off-shell couplings. The self-energy due to these couplings will not contribute in the renormalization of $S_F^{(\frac{3}{2})}$, but it will indeed change the non-resonant part. However, the effects due to these couplings can be expanded in powers of the momenta. So they will essentially look like *higher-order contact terms* without the Δ . This justifies the redundancy of these couplings. To ignore these couplings in a way that does not break term-by-term chiral symmetry, we can always combine ∂^μ with pion fields so that it becomes $\tilde{\partial}^\mu$. This indicates that those couplings with

$\tilde{\partial}^\mu$ or γ^μ contracted with Δ_μ can be ignored without breaking manifest chiral symmetry [62, 64]. For a concrete example of these results, see Appendix F.

To produce the $N \leftrightarrow \Delta$ transition currents, we construct the following lagrangians ($\hat{\nu} \leq 4$):

$$\mathcal{L}_{\Delta;N;\pi} = h_A \bar{\Delta}^{a\mu} T_a^{\dagger iA} \tilde{a}_{i\mu} N_A + C.C. , \quad (52)$$

$$\begin{aligned} \mathcal{L}_{\Delta;N;\text{background}} &= \frac{ic_{1\Delta}}{M} \bar{\Delta}_\mu^a \gamma_\nu \gamma^5 T_a^{\dagger iA} F_i^{(+)\mu\nu} N_A + \frac{ic_{3\Delta}}{M^2} \bar{\Delta}_\mu^a i\gamma^5 T_a^{\dagger iA} (\tilde{\partial}_\nu F^{(+)\mu\nu})_i N_A \\ &+ \frac{c_{6\Delta}}{M^2} \bar{\Delta}_\lambda^a \sigma_{\mu\nu} T_a^{\dagger iA} (\tilde{\partial}^\lambda \bar{F}^{(+)\mu\nu})_i N_A \\ &- \frac{d_{2\Delta}}{M^2} \bar{\Delta}_\mu^a T_a^{\dagger iA} (\tilde{\partial}_\nu F^{(-)\mu\nu})_i N_A - \frac{id_{4\Delta}}{M} \bar{\Delta}_\mu^a \gamma_\nu T_a^{\dagger iA} F_i^{(-)\mu\nu} N_A \\ &- \frac{id_{7\Delta}}{M^2} \bar{\Delta}_\lambda^a \sigma_{\mu\nu} T_a^{\dagger iA} (\tilde{\partial}^\lambda F^{(-)\mu\nu})_i N_A + C.C. , \end{aligned} \quad (53)$$

$$\begin{aligned} \mathcal{L}_{\Delta;N;\rho} &= \frac{ic_{1\Delta\rho}}{M} \bar{\Delta}_\mu^a \gamma_\nu \gamma^5 T_a^{\dagger iA} \rho_i^{\mu\nu} N_A + \frac{ic_{3\Delta\rho}}{M^2} \bar{\Delta}_\mu^a i\gamma^5 T_a^{\dagger iA} (\tilde{\partial}_\nu \rho^{\mu\nu})_i N_A \\ &+ \frac{c_{6\Delta\rho}}{M^2} \bar{\Delta}_\lambda^a \sigma_{\mu\nu} T_a^{\dagger iA} (\tilde{\partial}^\lambda \bar{\rho}^{\mu\nu})_i N_A + C.C. \end{aligned} \quad (54)$$

Terms omitted from these lagrangians are either redundant or are not relevant to our calculations [50].

4. Transition currents

It is easy to expect the validity of the following definitions:

$$\langle \Delta, a, p_\Delta | V^{i\mu} | N, A, p_N \rangle \equiv T_a^{\dagger iA} \bar{u}_{\Delta\alpha}(p_\Delta) \Gamma_V^{\alpha\mu}(q) u_N(p_N) , \quad (55)$$

$$\langle \Delta, a, p_\Delta | A^{i\mu} | N, A, p_N \rangle \equiv T_a^{\dagger iA} \bar{u}_{\Delta\alpha}(p_\Delta) \Gamma_A^{\alpha\mu}(q) u_N(p_N) . \quad (56)$$

Based on the lagrangians given previously, we find (note that $\sigma_{\mu\nu} \epsilon^{\mu\nu\alpha\beta} \propto i\sigma^{\alpha\beta} \gamma^5$)

$$\begin{aligned} \Gamma_V^{\alpha\mu} &= \frac{2c_{1\Delta}(q^2)}{M} (q^\alpha \gamma^\mu - \not{q} g^{\alpha\mu}) \gamma^5 + \frac{2c_{3\Delta}(q^2)}{M^2} (q^\alpha q^\mu - g^{\alpha\mu} q^2) \gamma^5 \\ &- \frac{8c_{6\Delta}(q^2)}{M^2} q^\alpha \sigma^{\mu\nu} i q_\nu \gamma^5 , \end{aligned} \quad (57)$$

$$\begin{aligned} \Gamma_A^{\alpha\mu} &= -h_A \left(g^{\alpha\mu} - \frac{q^\alpha q^\mu}{q^2 - m_\pi^2} \right) + \frac{2d_{2\Delta}}{M^2} (q^\alpha q^\mu - g^{\alpha\mu} q^2) - \frac{2d_{4\Delta}}{M} (q^\alpha \gamma^\mu - g^{\alpha\mu} \not{q}) \\ &- \frac{4d_{7\Delta}}{M^2} q^\alpha \sigma^{\mu\nu} i q_\nu , \end{aligned} \quad (58)$$

$$c_{i\Delta}(q^2) \equiv c_{i\Delta} + \frac{c_{i\Delta\rho}}{2g_\gamma} \frac{q^2}{q^2 - m_\rho^2} , \quad i = 1, 3, 6, \quad (59)$$

$$\begin{aligned} c_{1\Delta} &= 1.21, & c_{3\Delta} &= -0.61, & c_{6\Delta} &= -0.078, \\ \frac{c_{1\Delta\rho}}{g_\gamma} &= -4.58, & \frac{c_{3\Delta\rho}}{g_\gamma} &= 2.32, & \frac{c_{6\Delta\rho}}{g_\gamma} &= 0.30. \end{aligned} \quad (60)$$

Quite similar to the $c_{i\Delta}(q^2)$, we can also introduce axial-vector meson exchange into the axial transition current, which leads to a structure for the $d_{i\Delta}(q^2)$ that is similar to the vector transition current form factors. There is one subtlety associated with the realization of $h_A(q^2)$, which is the same as the one detailed in Appendix D for $G_A^{md}(q^2)$: with our lagrangian, we have a pion-pole contribution associated only with the h_A coupling, and all the higher-order terms contained in $\delta h_A(q^2) \equiv h_A(q^2) - h_A$ conserve the axial transition current. With the limited information about manifest chiral-symmetry breaking, we will ignore this subtlety and still use the form similar to the $c_{1\Delta}(q^2)$ to parameterize $h_A(q^2)$. The axial-vector meson couplings $h_{\Delta a_1}$ and $d_{i\Delta a_1}$ will be combinations of g_{a_1} and the coupling strength of $\Delta a_1 N$ interactions. So we have

$$h_A(q^2) \equiv h_A + h_{\Delta a_1} \frac{q^2}{q^2 - m_{a_1}^2}, \quad (61)$$

$$d_{i\Delta}(q^2) \equiv d_{i\Delta} + d_{i\Delta a_1} \frac{q^2}{q^2 - m_{a_1}^2}, \quad i = 2, 4, 7, \quad (62)$$

$$\begin{aligned} h_A &= 1.40, & d_{2\Delta} &= -0.087, & d_{4\Delta} &= 0.20, & d_{7\Delta} &= -0.04, \\ h_{\Delta a_1} &= -3.98, & d_{2\Delta a_1} &= 0.25, & d_{4\Delta a_1} &= -0.58, & d_{7\Delta a_1} &= 0.12. \end{aligned} \quad (63)$$

To determine the coefficients in the transition form factors shown in Eqs. (60) and (63), we will compare ours with the conventional ones used in the literature. In Refs. [30, 32] for example, the definition is

$$\begin{aligned} \langle \Delta, \frac{1}{2} | j_{cc+}^\mu | N, -\frac{1}{2} \rangle &\equiv \bar{u}_\alpha(p_\Delta) \left\{ \left[\frac{C_3^V}{M} (g^{\alpha\mu} \not{q} - q^\alpha \gamma^\mu) + \frac{C_4^V}{M^2} (q \cdot p_\Delta g^{\alpha\mu} - q^\alpha p_\Delta^\mu) \right. \right. \\ &\quad \left. \left. + \frac{C_5^V}{M^2} (q \cdot p_N g^{\alpha\mu} - q^\alpha p_N^\mu) \right] \gamma^5 \right. \\ &\quad \left. + \left[\frac{C_3^A}{M} (g^{\alpha\mu} \not{q} - q^\alpha \gamma^\mu) + \frac{C_4^A}{M^2} (q \cdot p_\Delta g^{\alpha\mu} - q^\alpha p_\Delta^\mu) \right. \right. \\ &\quad \left. \left. + C_5^A g^{\alpha\mu} + \frac{C_6^A}{M^2} q^\mu q^\alpha \right] \right\} u(p_N) \end{aligned} \quad (64)$$

$$\equiv -\sqrt{\frac{2}{3}} \bar{u}_\alpha(p_\Delta) (\Gamma_V^{\alpha\mu} + \Gamma_A^{\alpha\mu}) u(p_N), \quad (65)$$

where $\Gamma_V^{\alpha\mu}$ and $\Gamma_A^{\alpha\mu}$ are defined in Eqs. (55) and (56). The basis given above is known to be complete for the transition matrix element. The phenomenological form factors are listed

below [32]:

$$C_3^V(q^2) = \frac{2.13}{1 - (q^2/4M_V^2)} G_D(q^2), \quad (66)$$

$$C_4^V(q^2) = \frac{-1.51}{1 - (q^2/4M_V^2)} G_D(q^2), \quad (67)$$

$$C_5^V(q^2) = \frac{0.48}{1 - (q^2/0.776M_V^2)} G_D(q^2). \quad (68)$$

Here $G_D(q^2) \equiv \frac{1}{[1 - (q^2/M_V^2)]^2}$, and $M_V = 0.84$ GeV. (69)

$$C_3^A(q^2) = 0, \quad (70)$$

$$C_4^A(q^2) = -\frac{1}{4} C_5^A(q^2), \quad (71)$$

$$C_6^A(q^2) = C_5^A(q^2) \frac{M^2}{m_\pi^2 - q^2}, \quad (72)$$

$$C_5^A(q^2) = 1.14 \left(1 + \frac{1.21q^2}{2 \text{ GeV}^2 - q^2} \right) \frac{1}{[1 - (q^2/M_A^2)]^2}, \quad \text{where } M_A = 1.29 \text{ GeV}. \quad (73)$$

To equate the two different representations of the transition currents when $q^2 = 0$ and the baryons are on shell, we have:

$$c_{1\Delta} = \sqrt{\frac{3}{2}} \left[\frac{C_3^V}{2} + \frac{m - M}{2M} \frac{(C_4^V + C_5^V)}{2} \right], \quad (74)$$

$$c_{3\Delta} = \sqrt{\frac{3}{2}} \frac{(C_4^V - C_5^V)}{4}, \quad (75)$$

$$c_{6\Delta} = \sqrt{\frac{3}{2}} \frac{(C_4^V + C_5^V)}{16}. \quad (76)$$

$$h_A = \sqrt{\frac{3}{2}} C_5^A, \quad (77)$$

$$d_{2\Delta} = \sqrt{\frac{3}{2}} \frac{C_4^A}{4}, \quad (78)$$

$$d_{4\Delta} = -\sqrt{\frac{3}{2}} \left(\frac{C_3^A}{2} + \frac{m + M}{2M} \frac{C_4^A}{2} \right), \quad (79)$$

$$d_{7\Delta} = \sqrt{\frac{3}{2}} \frac{C_4^A}{8}. \quad (80)$$

To determine our own form factors, we assume that the relations above hold not only when $q^2 = 0$, but also in kinematic regimes with finite q^2 . It can be shown that at *low energy*, the differences in observables due to using the two bases, with these relations applied, are

negligible. This shows that our basis of invariants is also complete and partially justifies extending the preceding linear relations to kinematics with finite q^2 . Alternatively, all of the q^2 dependence of these $c_{i\Delta}$ and $d_{i\Delta}$ form factors can be realized in terms of meson dominance. We then require that the meson dominance form factors be as close as possible to the ones produced by the conventional form factors in Eqs. (74) to (80). However, when we compare our meson dominance form factors with those in literature, we clearly see the inadequacy of the leading-order meson dominance expressions above $Q^2 \approx 0.3 \text{ GeV}^2$.

III. FEYNMAN DIAGRAMS

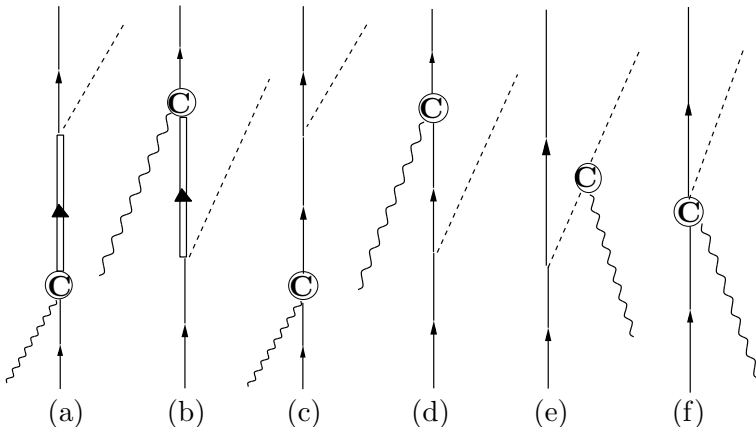


FIG. 1: Feynman diagrams for pion production. Here, **C** stands for various types of currents including vector, axial-vector, and baryon currents. Some diagrams may be zero for some specific type of current. For example, diagrams (a) and (b) will not contribute for the (isoscalar) baryon current. Diagram (e) will be zero for the axial-vector current. The pion-pole contributions are included in the vertex functions of the currents.

Tree-level Feynman diagrams for pion production due to the vector current, axial-vector current, and baryon current are shown in Fig. 1. In this section, we will begin to calculate different matrix elements for pion production and photon production. The Feynman diagrams for photon production can be viewed as diagrams in Fig. 1 with an outgoing π line changed to a γ line. It is easy to see that diagram (e) in Fig. 1 will not contribute to photon production, since there is no vertex connecting a pion and a photon.

A. Renormalized Δ propagator

Since the one-pion-loop self-energy has already been calculated in Ref. [45], we simply quote the result here:

$$S_F^{\mu\nu}(p) \equiv -\frac{\not{p} + m}{p^2 - m^2 - \Pi(\eta_p) + im\Gamma(p^2)} P^{(\frac{3}{2})\mu\nu} - \frac{1}{\sqrt{3}m} P_{12}^{(\frac{1}{2})\mu\nu} - \frac{1}{\sqrt{3}m} P_{21}^{(\frac{1}{2})\mu\nu} + \frac{2}{3m^2} (\not{p} + m) P_{22}^{(\frac{1}{2})\mu\nu} + O(\Gamma/m) \times \text{non-pole terms}, \quad (81)$$

$$\Gamma(p^2) = \frac{\pi}{12mp^4} \frac{h_A^2}{(4\pi f_\pi)^2} (p^2 + M^2 + 2Mm) \times [(p^2 - M^2)^2 - (p^2 + 3M^2)m_\pi^2] \sqrt{(p^2 - M^2)^2 - 4p^2 m_\pi^2}. \quad (82)$$

However, to make the calculation simpler, we will set $\Pi = 0$. We take $m = 1232$ MeV as the Breit–Wigner mass [65]. Note that Γ is implicitly associated with a factor of $\Theta[p^2 - (M + m_\pi)^2]$.

A few words on the $1/p^2$ singularities in the projection operators are in order here. (See Appendix E.) When the Δ is in the s channel, we never see these singularities, since p^2 is timelike. When the Δ is in other channels, for $p^2 \geq (m_\pi + M)^2$, we never see the singularities. For $p^2 \leq (m_\pi + M)^2$ and hence $\Gamma(p^2) = 0$, the apparent singularities are actually canceled out in our approximation scheme. It can be easily checked that if we set $\Pi = 0$, then when $\Gamma = 0$, $S_F^{\mu\nu}(p) \rightarrow S_F^{0\mu\nu}(p)$, so no singularities will appear. This is the advantage of setting $\Pi = 0$.

We have to remember, however, that the whole calculation is valid only in the low-energy limit, and in this limit, we would not see a Δ in the u channel that is far off shell, because both q and k_π are tiny. Hence the $1/p^2$ singularities should not be a problem in low-energy effective theory from a very general perspective.

B. Power counting of Feynman diagrams (ν) [66]

First let's outline the calculation of the interaction amplitude M . Consider CC pion production (in the one-weak-boson-exchange approximation):

$$M = 4\sqrt{2} G_F V_{ud} \langle J_{Li\mu}^{(lep)} \rangle \langle J_L^{(had)i\mu} \rangle_\pi, \quad (83)$$

where $i = +1, -1$. In Eq. (83), G_F is the Fermi constant, V_{ud} is the CKM matrix element corresponding to u and d quark mixing, $\langle J_{Li\mu}^{(lep)} \rangle \equiv \langle l(\bar{l}) | J_{Li\mu} | \nu_l(\bar{\nu}_l) \rangle$, and $\langle J_L^{(had)i\mu} \rangle_\pi \equiv \langle NB, \pi j | J_L^{i\mu} | NA \rangle$. $\langle J_{Li\mu}^{(lep)} \rangle$ is well known, so in the following, we focus on calculating $\langle J_L^{(had)i\mu} \rangle_\pi$.

For NC pion production:

$$M = 4\sqrt{2} G_F \langle J_{NC\mu}^{(lep)} \rangle \langle J_{NC}^{(had)\mu} \rangle_\pi, \quad (84)$$

where $\langle J_{NC\mu}^{(lep)} \rangle$ is the well-known leptonic neutral current matrix element, and $\langle J_{NC}^{(had)\mu} \rangle_\pi \equiv \langle NB, \pi j | J_{NC}^\mu | NA \rangle$. For NC photon production, we have a similar expression:

$$M = 4\sqrt{2} G_F \langle J_{NC\mu}^{(lep)} \rangle \langle J_{NC}^{(had)\mu} \rangle_\gamma, \quad (85)$$

where $\langle J_{NC}^{(had)\mu} \rangle_\gamma \equiv \langle NB, \gamma | J_{NC}^\mu | NA \rangle$.

Now consider the power counting for $\langle J^{(had)\mu} \rangle_{\pi(\gamma)}$ in Eqs. (83), (84), and (85). The order of the diagram (ν) is given by normal power counting [45]: $\nu = 2L + 2 - \frac{1}{2} E_n + \sum_i \#_i (\hat{\nu}_i - 2)$, where L is the number of loops, E_n is the number of external baryon lines, $\hat{\nu}_i \equiv d_i + \frac{1}{2} n_i + b_i$ is the order of the vertex ($\hat{\nu}$) defined in Sec. II B 2, and $\#_i$ is the number of times that particular vertex appears.

As pointed out in Ref. [66], by including Δ resonances in calculations, we have a new mass scale $\delta \equiv m - M \approx 300$ MeV. We must also consider the order of the Δ width Γ . Formally, it is counted as $O(Q^3/M^2)$; however, numerical calculations with Eq. (82) indicate that it should be counted as $O(Q^3/M^2 \times 10)$. Because of these two issues, we have to rethink the power counting of diagrams involving δ in two energy regimes. One is near the resonance, while the other is at lower energies, away from the resonance. In the resonance region, the Δ propagator scales like

$$S_F \sim \frac{1}{i\Gamma} + O\left(\frac{1}{M}\right) \approx \frac{1}{10i O(Q^3/M^2)} \approx \frac{1}{i O(Q^2/M)} \sim \frac{1}{O(Q)} \frac{M}{i O(Q)}, \quad (86)$$

where the $O(1/M)$ comes from non-pole terms. In the lower-energy region,

$$S_F \sim \frac{1}{2[\delta - O(Q)] - 10i O(Q^3/M^2)} + O\left(\frac{1}{M}\right) \sim \frac{1}{O(Q)} \frac{O(Q)}{\delta} + O\left(\frac{1}{M}\right) \approx \frac{1}{O(Q)} \frac{O(Q)}{M}. \quad (87)$$

So compared to the normal power counting mentioned above, in which the nucleon propagator scales as $1/O(Q)$, for diagrams involving one Δ in the s channel, we take $\nu \rightarrow \nu - 1$ in the resonance regime and $\nu \rightarrow \nu + 1$ away from the resonance. This partially justifies the strategy of incorporating non-resonant diagrams at low energies, while ignoring them in the resonance region when fitting the form factors in this region [31, 32].

C. CVC and PCAC

We will calculate matrix elements of currents and test the conservation of the vector current and the baryon current, and also partial conservation of the axial-vector current.

1. Diagram (a)

Diagram (a) in Fig. 1 leads to a vector current (k_π is the *outgoing* pion's momentum)

$$\langle V^{i\mu} \rangle_\pi = -\frac{i h_A}{f_\pi} T_{Bj}^a T_a^{\dagger iA} \bar{u}_f k_\pi^\lambda S_{F\lambda\alpha}(p) \Gamma_V^{\alpha\mu}(p; q, p_i) u_i. \quad (88)$$

Here $\Gamma_V^{\alpha\mu}(p; q, p_i)$ is defined in Eq. (55). Momentum conservation gives $p = q + p_i$, and $T_{jB}^a T_a^{\dagger iA} = \delta_j^i \delta_B^A - \frac{1}{3} (\tau_j \tau^i)_B^A = \frac{2}{3} \delta_j^i \delta_B^A - \frac{i}{3} \epsilon_j^{ik} (\tau_k)_B^A = \frac{2}{3} \delta_j^i \delta_B^A + \frac{i}{3} \epsilon_{jk}^i (\tau^k)_B^A$, where the subscript j denotes the isospin of the outgoing pion. Vector current conservation is obvious, and $\nu_{nr} \geq 3$ in the lower-energy region, while $\nu_r \geq 1$ in the resonance region. Here the higher-order terms in ν come from including form factors at the vertices.

The axial-vector current matrix element is

$$\langle A^{i\mu} \rangle_\pi = -\frac{i\hbar_A}{f_\pi} T_{Bj}^a T_a^{\dagger iA} \bar{u}_f k_\pi^\lambda S_{F\lambda\alpha}(p) \Gamma_A^{\alpha\mu}(p; q, p_i) u_i . \quad (89)$$

Here $\Gamma_A^{\alpha\mu}(p; q, p_i)$ is defined in Eq. (56). PCAC is also obvious, if we check the structure of $\Gamma_A^{\alpha\mu}$, and $\nu_{nr} \geq 2, \nu_r \geq 0$.

The baryon current matrix element is

$$\langle J_B^\mu \rangle_\pi = 0 . \quad (90)$$

Now we examine the NC matrix element $\langle J_{NC}^{(had)\mu} \rangle_\gamma$. First, based on the relations given in Eq. (25), we define

$$\Gamma_N^{\alpha\mu}(p; q, p_i) \equiv \left(\frac{1}{2} - \sin^2 \theta_w\right) \Gamma_V^{\alpha\mu}(p; q, p_i) + \frac{1}{2} \Gamma_A^{\alpha\mu}(p; q, p_i) , \quad (91)$$

$$\bar{\Gamma}_N^{\mu\alpha}(p_f; q, p) \equiv \gamma^0 \Gamma_N^{\dagger\alpha\mu}(p; -q, p_f) \gamma^0 , \quad (92)$$

$$\langle \Delta, a, p | J_{NC}^\mu(q) | N, A, p_i \rangle \equiv T_a^{\dagger 0A} \bar{u}_\alpha(p) \Gamma_N^{\alpha\mu}(p; q, p_i) u(p_i) , \quad (93)$$

$$\langle N, A, p_f | J_{NC}^\mu(q) | \Delta, a, p \rangle \equiv T_{0A}^a \bar{u}(p_f) \bar{\Gamma}_N^{\mu\alpha}(p_f; q, p) u_\alpha(p) . \quad (94)$$

Then we find [k is the outgoing photon's momentum and $\epsilon_\lambda^*(k)$ is its polarization]

$$\langle J_{NC}^\mu \rangle_\gamma = e T_{0B}^a T_a^{\dagger 0A} \bar{u}_f \epsilon_\lambda^*(k) \bar{\Gamma}_V^{\lambda\alpha}(p_f; -k, p) S_{F\alpha\beta}(p) \Gamma_N^{\beta\mu}(p; q, p_i) u_i . \quad (95)$$

CVC and PCAC are straightforward to verify here. For the vector current, $\nu_{nr} \geq 4, \nu_r \geq 2$, while for the axial-vector current, $\nu_{nr} \geq 3, \nu_r \geq 1$.

2. Diagram (b)

Diagram (b) in Fig. 1 leads to the vector current

$$\langle V^{i\mu} \rangle_\pi = -\frac{i\hbar_A}{f_\pi} T_B^{ai} T_{ja}^{\dagger A} \bar{u}_f \bar{\Gamma}_V^{\mu\alpha}(p_f; q, p) S_{F\alpha\lambda}(p) k_\pi^\lambda u_i . \quad (96)$$

Here $\bar{\Gamma}_V^{\mu\alpha}(p_f; q, p) \equiv \gamma^0 \Gamma_V^{\dagger\alpha\mu}(p; -q, p_f) \gamma^0$, $p = -q + p_f$, and $T_B^{ai} T_{aj}^{\dagger A} = \delta_j^i \delta_B^A - \frac{1}{3} (\tau^i \tau_j)_B^A = \frac{2}{3} \delta_j^i \delta_B^A - \frac{i}{3} \epsilon_{jk}^i (\tau^k)_B^A$. The conservation of the vector current is obvious, and $\nu_{nr} \geq 3$.

The axial-vector current matrix element is

$$\langle A^{i\mu} \rangle_\pi = -\frac{i\hbar_A}{f_\pi} T_B^{ai} T_{ja}^{\dagger A} \bar{u}_f \bar{\Gamma}_A^{\mu\alpha}(p_f; q, p) S_{F\alpha\lambda}(p) k_\pi^\lambda u_i . \quad (97)$$

Here $\bar{\Gamma}_A^{\mu\alpha}(p_f; q, p) \equiv \gamma^0 \Gamma_A^{\dagger\alpha\mu}(p; -q, p_f) \gamma^0$, $p = -q + p_f$, PCAC is again obvious, and $\nu_{nr} \geq 2$.

The baryon current matrix element is zero ($\langle J_B^\mu \rangle_\pi = 0$), and the NC current matrix element for photon production is

$$\langle J_{NC}^\mu \rangle_\gamma = e T_B^{a0} T_{a0}^{\dagger A} \bar{u}_f \bar{\Gamma}_N^{\mu\alpha}(p_f; q, p) S_{F\alpha\beta}(p) \Gamma_V^{\beta\lambda}(p; -k, p_i) \epsilon_\lambda^*(k) u_i . \quad (98)$$

Both CVC and PCAC are obvious here. For the vector current, $\nu_{nr} \geq 4$, while for the axial-vector current, $\nu_{nr} \geq 3$.

3. Diagrams (c) and (d)

These two diagrams lead to a vector current

$$\begin{aligned} \langle V^{i\mu} \rangle_\pi &= -\frac{ig_A}{f_\pi} \langle B | \frac{\tau_j}{2} \frac{\tau^i}{2} | A \rangle \bar{u}_f \not{k}_\pi \gamma^5 S_F(p) \Gamma_V^\mu(q) u_i \\ &\quad - \frac{ig_A}{f_\pi} \langle B | \frac{\tau^i}{2} \frac{\tau_j}{2} | A \rangle \bar{u}_f \Gamma_V^\mu(q) S_F(p) \not{k}_\pi \gamma^5 u_i . \end{aligned} \quad (99)$$

Here $S_F(p) = S_F(q + p_i)$ is the nucleon propagator, $\Gamma_V^\mu(q)$ has been defined in Eq. (27), and $\nu \geq 1$. To prove CVC, one must consider diagrams (c), (d), (e), and (f) together.

For the axial-vector current, we find

$$\begin{aligned} \langle A^{i\mu} \rangle_\pi &= -\frac{ig_A}{f_\pi} \langle B | \frac{\tau_j}{2} \frac{\tau^i}{2} | A \rangle \bar{u}_f \not{k}_\pi \gamma^5 S_F(p) \Gamma_A^\mu(q) u_i \\ &\quad - \frac{ig_A}{f_\pi} \langle B | \frac{\tau^i}{2} \frac{\tau_j}{2} | A \rangle \bar{u}_f \Gamma_A^\mu(q) S_F(p) \not{k}_\pi \gamma^5 u_i . \end{aligned} \quad (100)$$

Here, $\Gamma_A^\mu(q)$ has been defined in Eq. (40), PCAC is obvious, and $\nu \geq 1$.

For the baryon current we have

$$\begin{aligned} \langle J_B^\mu \rangle_\pi &= -\frac{ig_A}{f_\pi} \langle B | \frac{\tau_j}{2} | A \rangle \bar{u}_f \not{k}_\pi \gamma^5 S_F(p) \Gamma_B^\mu(q) u_i \\ &\quad - \frac{ig_A}{f_\pi} \langle B | \frac{\tau_j}{2} | A \rangle \bar{u}_f \Gamma_B^\mu(q) S_F(p) \not{k}_\pi \gamma^5 u_i . \end{aligned} \quad (101)$$

Here, $\Gamma_B^\mu(q)$ has been defined in Eq. (30). It is easy to see that the baryon current is conserved and that $\nu \geq 1$.

Finally, for NC photon production, we get

$$\begin{aligned} \langle J_{NC}^\mu \rangle_\gamma &= e \bar{u}_f \epsilon_\lambda^*(k) \left(\left(\frac{\tau^0}{2} \right)_B^C \Gamma_V^\lambda(-k) + \frac{\delta_B^C}{2} \Gamma_B^\lambda(-k) \right) S_F(p) \\ &\quad \times \left(\left(\frac{\tau^0}{2} \right)_C^A \left[\left(\frac{1}{2} - \sin^2 \theta_w \right) \Gamma_V^\mu(q) + \frac{1}{2} \Gamma_A^\mu(q) \right] - \frac{\delta_C^A}{2} \sin^2 \theta_w \Gamma_B^\mu(q) \right) u_i \\ &\quad + e \bar{u}_f \left(\left(\frac{\tau^0}{2} \right)_B^C \left[\left(\frac{1}{2} - \sin^2 \theta_w \right) \Gamma_V^\mu(q) + \frac{1}{2} \Gamma_A^\mu(q) \right] - \frac{\delta_B^C}{2} \sin^2 \theta_w \Gamma_B^\mu(q) \right) \\ &\quad \times S_F(p) \epsilon_\lambda^*(k) \left(\left(\frac{\tau^0}{2} \right)_C^A \Gamma_V^\lambda(-k) + \frac{\delta_C^A}{2} \Gamma_B^\lambda(-k) \right) u_i , \end{aligned} \quad (102)$$

where we use the shorthand

$$\left(\frac{\tau^0}{2} \right)_B^A = \langle B | \frac{\tau^0}{2} | A \rangle . \quad (103)$$

One can verify the conservation of the vector current and the baryon current, as well as the partial conservation of the axial-vector current. For all three currents, power counting gives $\nu \geq 1$. However, this naive power counting does not give an accurate comparison between the Δ contributions and the N contributions at low energies, as we discuss below.

4. Diagrams (e) and (f)

The two diagrams lead to a vector current

$$\langle V^{i\mu} \rangle_\pi = \frac{g_A}{2f_\pi} \epsilon^i{}_{jk} (\tau^k)_B^A \frac{P_V^\mu(q, k_\pi)}{(q - k_\pi)^2 - m_\pi^2} \bar{u}_f (\not{q} - \not{k}_\pi) \gamma^5 u_i \quad (104)$$

$$+ \frac{\epsilon^i{}_{jk}}{f_\pi} \langle B | \frac{\tau^k}{2} | A \rangle \bar{u}_f \Gamma_{V\pi}^\mu(q, k_\pi) u_i . \quad (105)$$

Here, $P_V^\mu(q, k_\pi)$ is defined in Eq. (46), $\Gamma_{V\pi}^\mu(q, k_\pi)$ is defined in Eq. (42), and $\nu \geq 1$. Finally, we can combine diagrams (c), (d), (e), and (f) to get vector current conservation.

For the axial-vector current, diagram (e) does not contribute, and we find

$$\langle A^{i\mu} \rangle_\pi = \frac{\epsilon^i{}_{jk}}{f_\pi} \langle B | \frac{\tau^k}{2} | A \rangle \bar{u}_f \Gamma_{A\pi}^\mu(q, k_\pi) u_i + \frac{\epsilon^i{}_{jk}}{f_\pi} \langle B | \frac{\tau^k}{2} | A \rangle \frac{q^\mu}{q^2 - m_\pi^2} \bar{u}_f \frac{(\not{q} + \not{k}_\pi)}{2} u_i \quad (106)$$

$$+ \frac{\epsilon^i{}_{jk}}{f_\pi} \langle B | \frac{\tau^k}{2} | A \rangle 4\kappa_\pi \bar{u}_f \left(\frac{\sigma^{\mu\nu} i k_{\pi\nu}}{2M} + \frac{q^\mu}{q^2 - m_\pi^2} \frac{\sigma^{\alpha\beta} i k_{\pi\alpha} q_\beta}{2M} \right) u_i \quad (107)$$

$$+ \frac{\delta_j^i}{f_\pi} \delta_B^A 4\beta_\pi \frac{1}{M} \left(-i k_\pi^\mu + \frac{i q \cdot k_\pi q^\mu}{q^2 - m_\pi^2} \right) \bar{u}_f u_i \quad (108)$$

$$+ \frac{\delta_j^i}{f_\pi} \delta_B^A \frac{-i\kappa_1}{4} \frac{1}{M^2} \bar{u}_f \left(q_\nu (p_f + p_i) \{\nu\gamma^\mu\} - \frac{q \cdot (p_f + p_i) q^\mu}{q^2 - m_\pi^2} (\not{q} + \not{k}_\pi) \right) u_i . \quad (109)$$

Here, $\Gamma_{A\pi}^\mu(q, k_\pi)$ is given in Eq. (33) and leads to a $\nu \geq 1$ contribution. The contributions due to κ_π , β_π , and κ_1 are at $\nu = 2$. It is easy to check that PCAC holds.

For the baryon current, diagrams (e) and (f) do not contribute at order $\nu = 1$: $\langle J_B^\mu \rangle_\pi = 0$.

For the NC photon production matrix element we find

$$\begin{aligned} \langle J_{NC}^\mu \rangle_\gamma &= \delta_B^A \frac{-ie c_1}{M^2} \epsilon^{\mu\nu\alpha\beta} \bar{u}_f \gamma_\nu k_\alpha \epsilon_\beta^*(k) u_i \\ &+ \delta_B^A \frac{-ie c_1 q^\mu}{M^2 (q^2 - m_\pi^2)} \epsilon^{\lambda\nu\alpha\beta} \bar{u}_f \gamma_\lambda q_\nu k_\alpha \epsilon_\beta^*(k) u_i \\ &+ \left(\frac{\tau^0}{2} \right)_B^A \frac{-ie e_1}{2M^2} \epsilon^{\mu\nu\alpha\beta} \bar{u}_f \gamma_\nu k_\alpha \epsilon_\beta^*(k) u_i \\ &+ \left(\frac{\tau^0}{2} \right)_B^A \frac{-ie e_1 q^\mu}{2M^2 (q^2 - m_\pi^2)} \epsilon^{\lambda\nu\alpha\beta} \bar{u}_f \gamma_\lambda q_\nu k_\alpha \epsilon_\beta^*(k) u_i . \end{aligned} \quad (110)$$

It is straightforward to see that PCAC is satisfied. Here $\nu = 3$; for $\nu < 3$, there are no contact vertices contributing to the NC photon production channel. By power counting, we expect that at low energy, these terms can be neglected compared to the $\nu = 1$ terms. However, as claimed in Ref. [67], these contact vertices have possible high-energy extrapolations due to the anomalous decays of the ω and ρ . According to Ref. [67], these terms may play an important role in coherent photon production. However, we must realize that the constants c_1 and e_1 can only be fixed by experiment, and it is not clear that only anomalous meson decay will contribute to these operators at low energy. As shown in the lagrangian, we can

construct meson dominance by coupling mesons instead of photons to the vertex. Moreover, these terms are also the same as operators induced by the off-shell parameters in the Δ lagrangian.

IV. RESULTS

In this section, after introducing the kinematics, we will discuss our results for CC and NC pion production, and also NC photon production, and compare them with available data whenever possible. Aiming at the excessive events in the MiniBooNE experiment, we will focus on the scattering of ν_μ and $\bar{\nu}_\mu$ off nucleons with $E_{\nu,\bar{\nu}} \leq 0.5$ GeV.

A. Kinematics

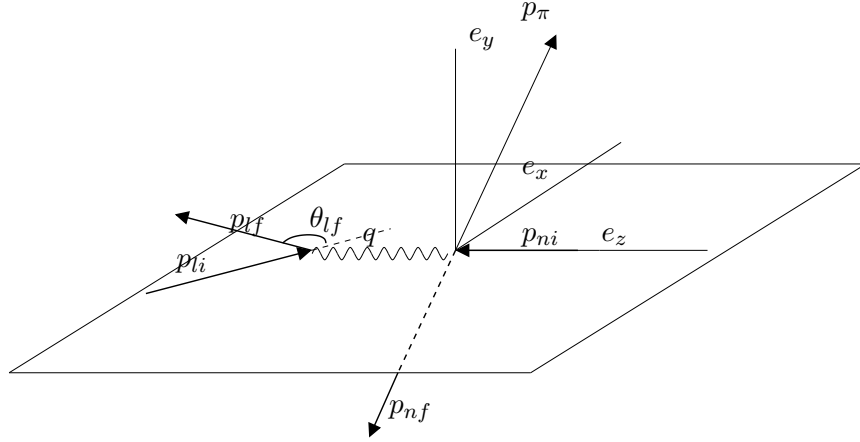


FIG. 2: The configuration in the isobaric frame.

Figure 2 shows the configuration in the isobaric frame, i.e., the cm frame of the final nucleon and pion. The momenta are measured in this frame, except those labeled as p^L , which denotes a momentum measured in the Lab frame with the initial nucleon stationary. Detailed analysis of the kinematics is given in Appendix G. The expression for the total cross section for this process is ($|\overline{M}|^2$ is the averaged total interaction amplitude squared.)

$$\begin{aligned}
\sigma &= \int \frac{|\overline{M}|^2}{4|p_{li}^L \cdot p_{ni}^L|} (2\pi)^4 \delta^{(4)}\left(\sum_i p_i\right) \frac{d^3 \vec{p}_{if}^L}{(2\pi)^3 2E_{if}^L} \frac{d^3 \vec{p}_{\pi}^L}{(2\pi)^3 2E_{\pi}^L} \frac{d^3 \vec{p}_{nf}^L}{(2\pi)^3 2E_{nf}^L} \\
&= \int \frac{|\overline{M}|^2}{32M_n} \frac{1}{(2\pi)^5} \frac{|\vec{p}_{\pi}|}{E_{\pi} + E_{nf}} \frac{|\vec{p}_{if}^L|}{|\vec{p}_{li}^L|} d\Omega_{\pi} dE_{if}^L d\Omega_{if}^L \\
&= \int \frac{|\overline{M}|^2}{64M_n^2} \frac{1}{(2\pi)^5} \frac{|\vec{p}_{\pi}|}{E_{\pi} + E_{nf}} \frac{\pi}{|\vec{p}_{li}^L| E_{li}^L} d\Omega_{\pi} dM_{\pi n}^2 dQ^2 .
\end{aligned} \tag{111}$$

Based on the equations in Appendix G, we can make the following estimates:

For CC pion production:

- When $E_\nu^L = 0.4 \text{ GeV}$, $(M_{\pi n})_{max} \cong 1.17 \text{ GeV}$, $Q_{max}^2 \cong 0.2 \text{ GeV}^2$.
- When $E_\nu^L = 0.5 \text{ GeV}$, $(M_{\pi n})_{max} \cong 1.24 \text{ GeV}$, $Q_{max}^2 \cong 0.3 \text{ GeV}^2$.

We can see that above $E_\nu^L = 0.4 \text{ GeV}$, the interaction begins to be dominated by the Δ resonance. However, when $E_\nu^L = 0.75 \text{ GeV}$, $(M_{\pi n})_{max} \cong 1.4 \text{ GeV}$, and higher resonances, for example $P_{11}(1440)$, may play a significant role. The exception is that for $\nu_\mu + p \rightarrow \mu^- + p + \pi^+$, only $I = 3/2$ can contribute, and the next resonance in this channel is the $\Delta(1600)$, which is accessible only when $E_\nu^L \geq 1.8 \text{ GeV}$.

For NC pion production:

- When $E_\nu^L = 0.3 \text{ GeV}$, $(M_{\pi n})_{max} \cong 1.2 \text{ GeV}$, $Q_{max}^2 \cong 0.1 \text{ GeV}^2$.
- When $E_\nu^L = 0.5 \text{ GeV}$, $(M_{\pi n})_{max} \cong 1.35 \text{ GeV}$, $Q_{max}^2 \cong 0.3 \text{ GeV}^2$.

Here, we can see that above $E_\nu^L = 0.3 \text{ GeV}$, the interaction begins to be dominated by the Δ . However, when $E_\nu^L = 0.6 \text{ GeV}$, $(M_{\pi n})_{max} \cong 1.4 \text{ GeV}$, and higher resonances may play a significant role.

For NC photon production ($E_\gamma^L \geq 0.2 \text{ GeV}$):

- When $E_\nu^L = 0.3 \text{ GeV}$, $(M_{\gamma n})_{max} \cong 1.2 \text{ GeV}$, $Q_{max}^2 \cong 0.1 \text{ GeV}^2$.
- When $E_\nu^L = 0.5 \text{ GeV}$, $(M_{\gamma n})_{max} \cong 1.35 \text{ GeV}$, $Q_{max}^2 \cong 0.3 \text{ GeV}^2$.

Here, we expect the Δ to dominate when $E_\nu^L \geq 0.3 \text{ GeV}$. But, similar to the case of NC pion production, higher resonances may need to be considered when $E_\nu^L \geq 0.6 \text{ GeV}$.

From the analysis outlined above, we can expect our EFT to be valid at $E_\nu^L \leq 0.5 \text{ GeV}$, since only the Δ resonance can be excited, and $Q^2 \leq 0.3 \text{ GeV}^2$, so that meson dominance works for various currents' form factors [20]. To go beyond this energy regime when we show our results, we will require $M_{\pi n} \leq 1.4 \text{ GeV}$ and will use standard phenomenological form factors that work when $Q^2 \geq 0.3 \text{ GeV}^2$.

B. CC pion production

In this section, we will compare CC pion neutrino production results with ANL [34] and BNL [35] measurements. In both experiments, the targets are hydrogen and deuterium. (All the other experiments use much heavier nuclear targets in (anti)neutrino scattering, and to explain this, we must examine many-body effects.) The beam is ν_μ , the average energy of which is 1 GeV and 1.6 GeV for ANL and BNL, respectively. In the ANL data, there is a cut on the invariant mass of the pion and final nucleon system: $M_{\pi n} \leq 1.4 \text{ GeV}$. In the BNL data, there is no such cut. Based on the phase-space analysis discussed above, this cut clearly reduces the number of events when E_ν is above $0.5 \sim 0.6 \text{ GeV}$. Since the data stretch above this limit, in the first three figures: 3, 4, and 5, we show our conventional form factor ('cff') calculations with the $M_{\pi n}$ constraint. That is, for F^{md} , G^{md} , c_Δ , and d_Δ we substitute the conventional form factors used in the literature [32]. Then we apply our lagrangian to the meson dominance form factor ('mdff') calculations. As we have already concluded that this 'mdff' approach is inadequate above $E_\nu = 0.5 \text{ GeV}$, in the following figures: 6, 7, 8, 9, 10, and 11, we show the 'mdff' results with $E_\nu \leq 0.5 \sim 0.6 \text{ GeV}$, for which $M_{\pi n} \leq 1.4 \text{ GeV}$ holds automatically. Since we believe the EFT is applicable in this low-energy regime, in these figures, we show results including Feynman diagrams up to order $\nu = 1$ and $\nu = 2$.

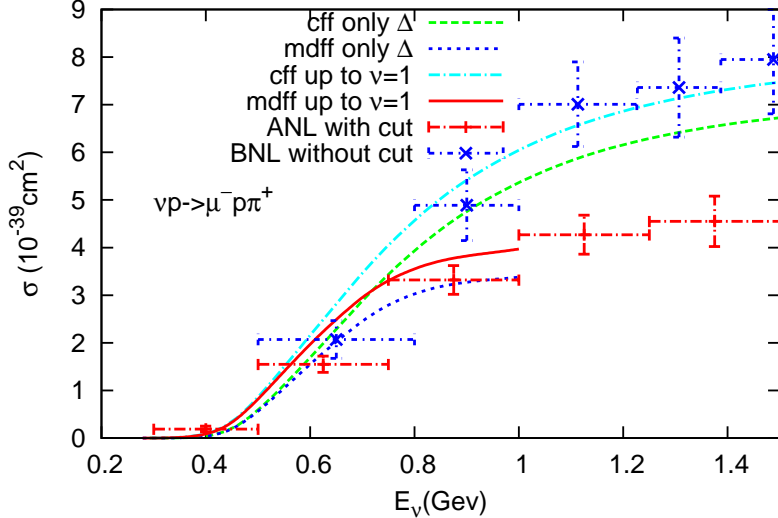


FIG. 3: Total cross section for $\nu_\mu + p \rightarrow \mu^- + p + \pi^+$. ‘Only Δ ’ indicates that only diagrams with Δ (both s and u channels) are included. ‘Up to $\nu = 1$ ’ includes all the diagrams at leading order. The code ‘cff’ indicates that the calculations are done with conventional form factors, while ‘mdff’ indicates the calculations are based on the EFT lagrangian with meson dominance. In the ANL data, $M_{\pi n} \leq 1.4$ GeV is applied, while no such cut is applied in the BNL data. For all calculations, $M_{\pi n} \leq 1.4$ GeV is applied.

In Fig. 3, we show the data and calculations for $\nu_\mu + p \rightarrow \mu^- + p + \pi^+$. The ANL data is systemically smaller than the BNL data, due to enforcing the $M_{\pi n}$ constraint at ANL. As mentioned above, we make use of the conventional form factors and include in the ‘cff only Δ ’ calculation the Feynman diagrams with the Δ in both s and u channels and in the ‘cff up to $\nu = 1$ ’ all the Feynman diagrams up to leading order. These two calculations are quite similar to those done in Ref. [30]. Indeed, our results are consistent with theirs for the conventional value of C_5^A . (In Ref. [30], only the s channel contribution is included in the calculation with ‘only Δ ’.) Next, we apply our lagrangian in the ‘mdff’ calculations, in which form factors are realized in terms of meson dominance. In Fig. 3, we show both the result with only Δ diagrams and the result with all the leading-order diagrams in the ‘mdff’ calculations, so that we can compare the ‘mdff’ approach with the ‘cff’ approach.

First, we can see that both ‘cff’ and ‘mdff’ with only Δ diagrams are consistent with the data at $E_\nu \leq 0.5$ GeV. Introducing other diagrams up to order $\nu = 1$ is still allowed by the data at low energy, although they indeed increase the cross section noticeably. Second, the two approaches with the same diagrams begin to differ from each other beyond $E_\nu = 0.5$ GeV, which is also consistent with the analysis of phase space and the discussion of the validity of meson dominance. In Ref. [30], a reduced $C_5^A(0)$ is introduced, primarily to reduce the calculated cross sections above $E_\nu = 1$ GeV. However, since we are only concerned with the $E_\nu \leq 0.5$ GeV region, in which we see satisfactory agreement between our calculations and the data, we will stick to the $C_5^A(0)$ fitted from the Δ free width in the framework of our EFT lagrangian. Furthermore, in the original spectrum-averaged $d\sigma/dQ^2$ data of ANL [34], the contributions from $E_\nu \leq 0.5$ GeV neutrinos are excluded, so comparing calculations with data at low energy is not feasible at this stage, and we will not show our $d\sigma/dQ^2$ here.

In Figs. 4 and 5, we show the data and calculations for $\nu_\mu + n \rightarrow \mu^- + n + \pi^+$ and $\nu_\mu +$

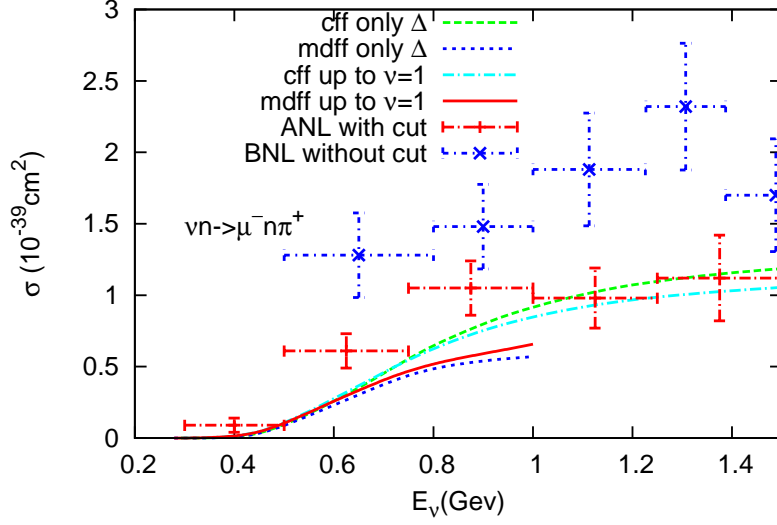


FIG. 4: Total cross section for $\nu_\mu + n \rightarrow \mu^- + n + \pi^+$. The curves are defined as in Fig. 3.

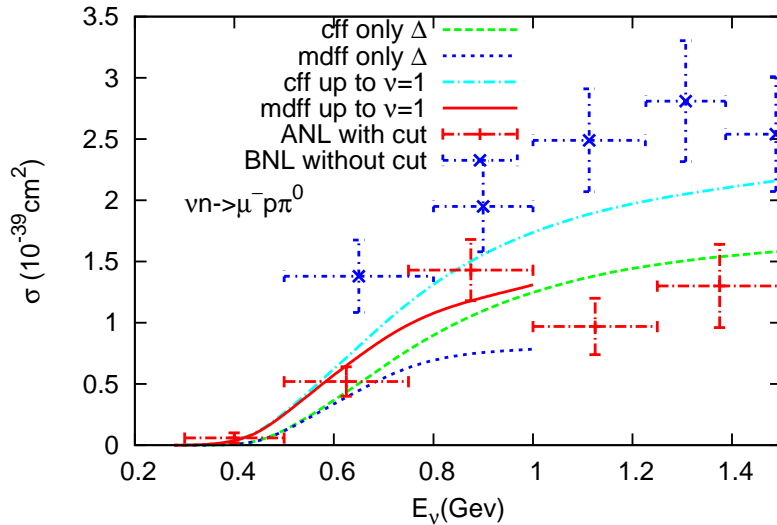


FIG. 5: Total cross section for $\nu_\mu + n \rightarrow \mu^- + p + \pi^0$. The curves are defined as in Fig. 3.

$n \rightarrow \mu^- + p + \pi^0$. We can see that the situations in these two processes are quite similar to the one in Fig. 3: the results of the ‘cff’ and ‘mdff’ approaches are consistent with the data at low energy. Again the differences between the two approaches with the same diagrams begin to show up when the neutrino energy goes beyond 0.5 GeV. Although the pion production is still dominated by the Δ , other diagrams introduce significant contributions, which violate the naive estimate of the ratio of the three channels’ cross sections based on isospin symmetry and Δ dominance.

In Figs. 6, 7, 8, 9, 10, and 11, we begin to investigate the convergence of our calculations in different channels in neutrino and antineutrino scattering. We show the ‘mdff’ calculations based on our EFT lagrangian up to different orders. We see that the power counting makes sense systematically in different channels: including N and contact terms up to $\nu = 1$

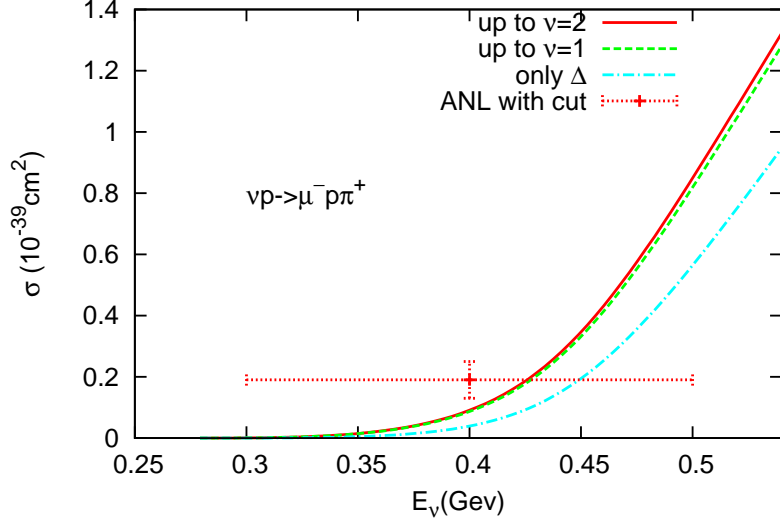


FIG. 6: Total cross section for $\nu_\mu + p \rightarrow \mu^- + p + \pi^+$. ‘Only Δ ’ indicates that only diagrams with Δ (both s and u channels) are included. ‘Up to $\nu = 1$ ’ includes all the diagrams at leading order. ‘Up to $\nu = 2$ ’ includes higher-order contact terms, whose couplings are from Ref. [68]. In the ANL data, $M_{\pi n} \leq 1.4$ GeV. For calculations, $M_{\pi n} \leq 1.4$ GeV is applied.

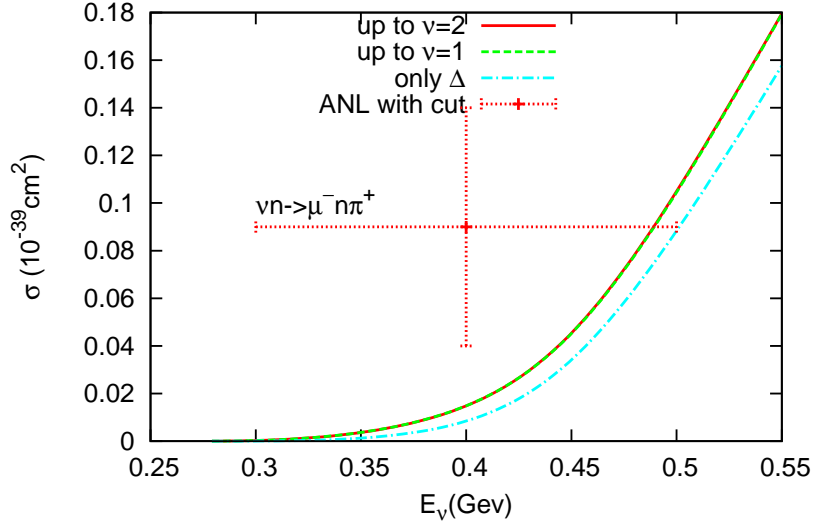


FIG. 7: Total cross section for $\nu_\mu + n \rightarrow \mu^- + n + \pi^+$. The curves are defined as in Fig. 6.

changes the ‘only Δ ’ calculation non-negligibly. (Far away from resonance, we see that the Δ contribution is not dominant compared to other diagrams, and it begins to dominate around 0.4 GeV. This is consistent with the power counting discussed in Sec. III B). However, the $\nu = 2$ terms do not change the ‘up to $\nu = 1$ ’ results significantly. This partially justifies the use of meson dominance, which automatically includes higher-order terms. All the calculations of neutrino scattering are consistent with the limited data from ANL. We can see that the cross section for antineutrino scattering is generally smaller than that of neutrino scattering, due to the relative sign chosen between $V^{i\mu}$ and $A^{i\mu}$ in the Feynman diagrams

with Δ . The signs between $V^{i\mu}$ and $A^{i\mu}$ in other diagrams is well defined in our lagrangian. However, the relative sign between currents due to the Δ and other diagrams is not well constrained by the available data in our framework, as indicated in Ref. [30]. Here we rely on the sign of h_A fitted in pion–nucleon scattering [68] to set the sign between the Δ current and the background contribution, as shown in Eqs. (74) to (80).

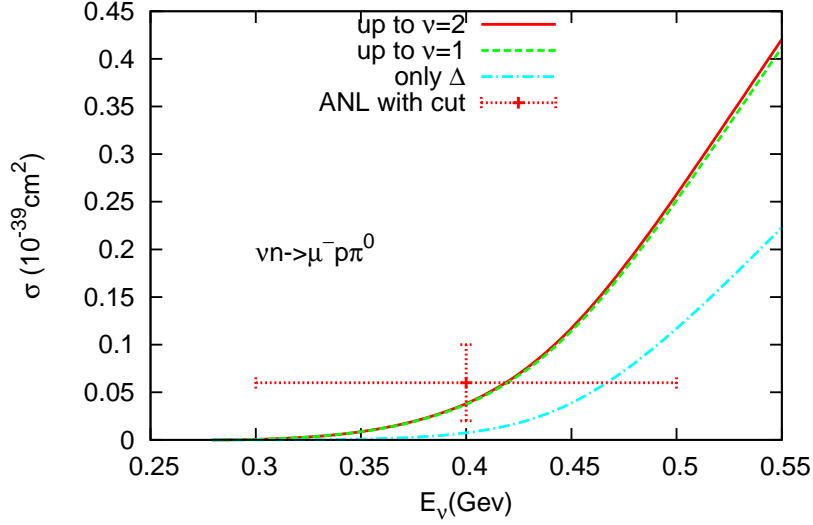


FIG. 8: Total cross section for $\nu_\mu + n \rightarrow \mu^- + p + \pi^0$. The curves are defined as in Fig. 6.

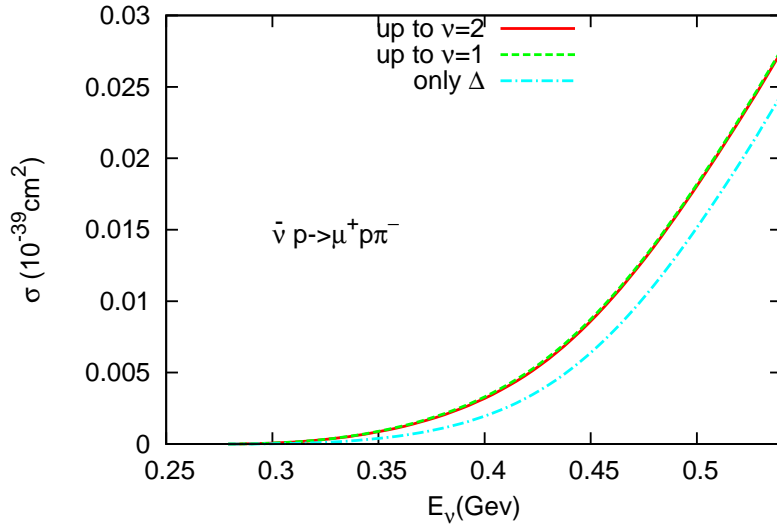


FIG. 9: Total cross section for $\bar{\nu}_\mu + p \rightarrow \mu^+ + p + \pi^-$. The curves are defined as in Fig. 6.

C. NC pion production

In this section, we discuss the results for NC pion production in (anti)neutrino scattering. In Figs. 12 and 13, the results in the ‘mdff’ approach including diagrams of different orders

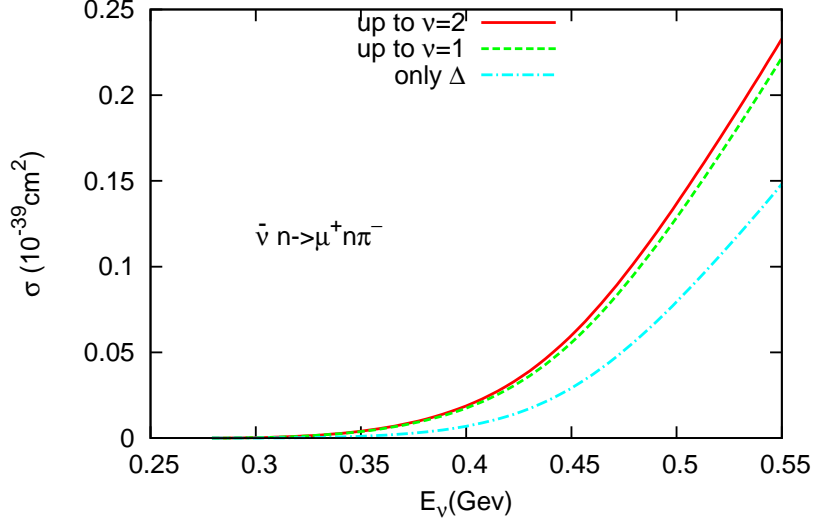


FIG. 10: Total cross section for $\bar{\nu}_\mu + n \rightarrow \mu^+ + n + \pi^-$. The curves are defined as in Fig. 6.

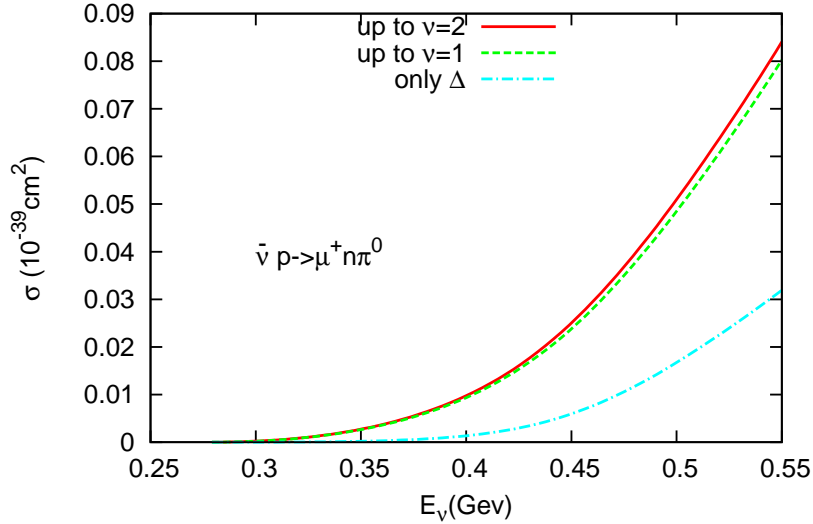


FIG. 11: Total cross section for $\bar{\nu}_\mu + p \rightarrow \mu^+ + n + \pi^0$. The curves are defined as in Fig. 6.

are shown for neutrino scattering, while the results for antineutrino scattering are shown in Figs. 14 and 15. The channels are explained in each plot.

Since all of the available data for NC pion production are spectrum averaged, and neutrinos with $E_\nu \leq 0.5$ GeV have small weight in such spectrum integrated analyses, we will not compare our results with data. In other words, current data does not put strong constraints on the NC pion production in this energy regime.

Nevertheless, we clearly see the convergence of our calculations; introducing the $\nu = 2$ terms does not change the total cross section significantly. However, we also see the violation of isospin symmetry in the ‘up to $\nu = 1$ ’ and ‘up to $\nu = 2$ ’ calculations in each plot, if we compare each pair of channels in every plot, namely, Figs. 12, 13, 14, and 15. In principle, if there is no baryon current contribution in NC production, we should see that the two

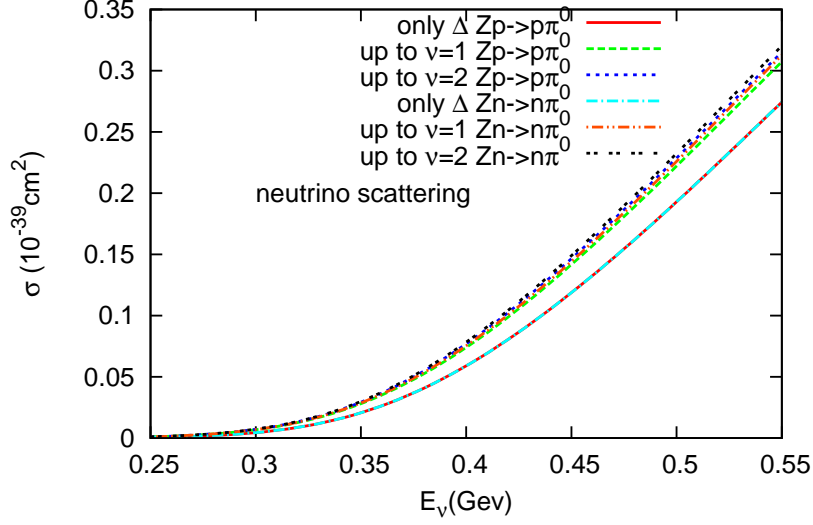


FIG. 12: Total cross section for NC π^0 production due to neutrino scattering. The curves are defined as in Fig. 6, and the channels are also indicated.

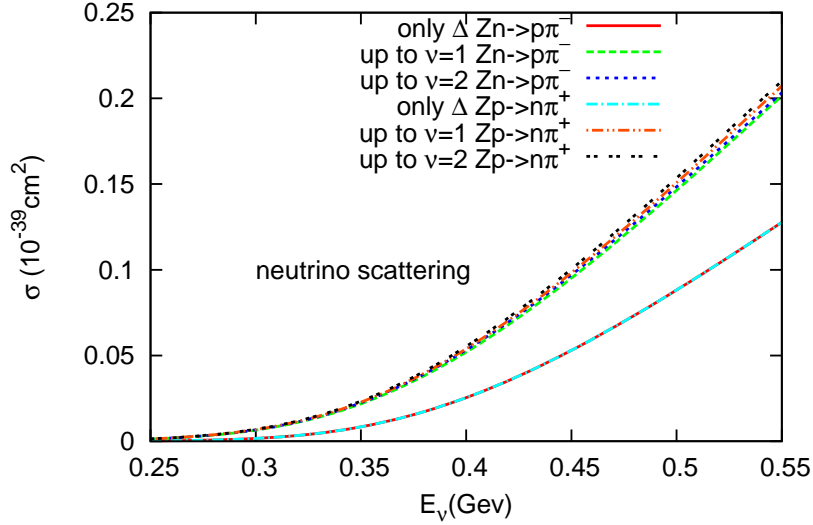


FIG. 13: Total cross section for NC π^\pm production due to neutrino scattering. The curves are defined as in Fig. 6, and the channels are also indicated.

channels yield the same results in each plot. For example, isospin symmetry implies

$$\langle p, \pi^0 | V^{0\mu}, A^{0\mu} | p \rangle = \langle n, \pi^0 | V^{0\mu}, A^{0\mu} | n \rangle, \quad (112)$$

$$\langle p, \pi^0 | J_B^\mu | p \rangle = -\langle n, \pi^0 | J_B^\mu | n \rangle. \quad (113)$$

So with ‘only Δ ’, we will not see the difference between the two cross sections, since the (isoscalar) baryon current cannot induce transitions from N to Δ . After introducing background terms, which contain contributions from the baryon current, we would expect the results for the two processes to be different, as confirmed in Fig. 12. This analysis is applicable to the other plots.

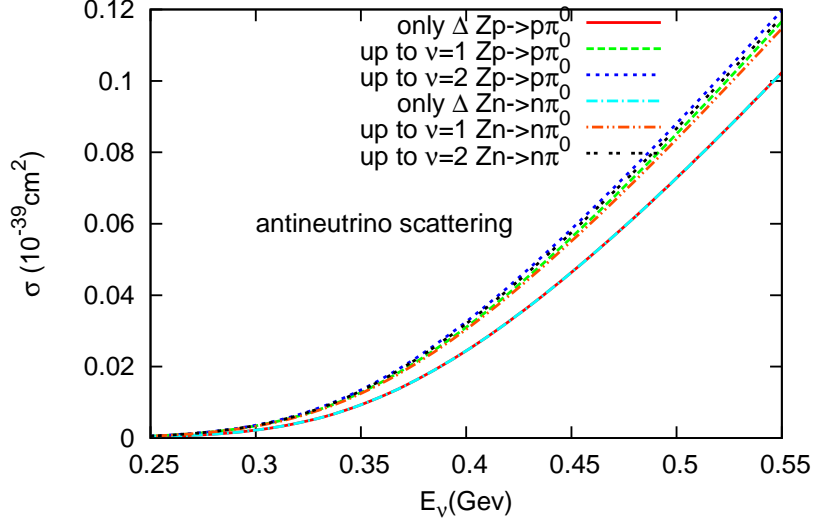


FIG. 14: Total cross section for NC π^0 production due to antineutrino scattering. The curves are defined as in Fig. 6, and the channels are also indicated.

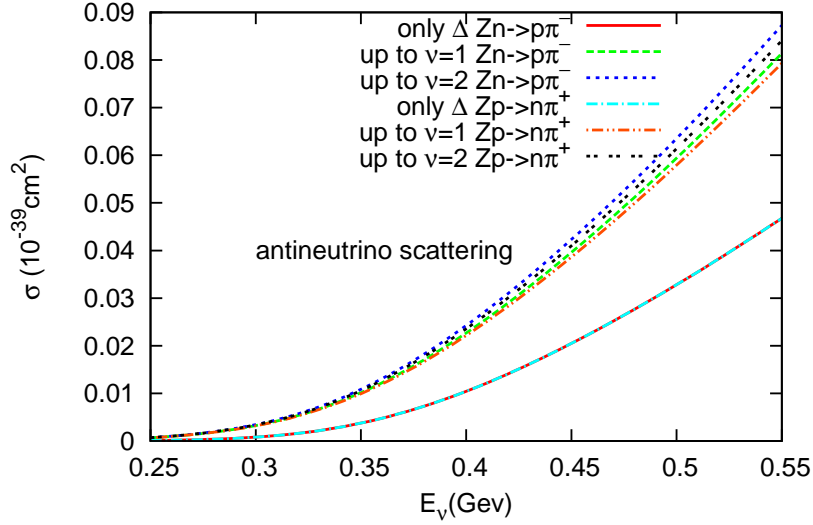


FIG. 15: Total cross section for NC π^\pm production due to antineutrino scattering. The curves are defined as in Fig. 6, and the channels are also indicated.

D. NC photon production

In this section we focus on NC photon production. Besides NC π^0 production, this process is another important background in neutrino experiments. As we are ultimately concerned with the excessive events in the MiniBooNE experiment [1], we focus on $E_\nu \leq 0.5$ GeV, as mentioned in the beginning of this paper. One important difference between NC photon production and CC and NC pion production, is that all of the $\nu = 2$ terms do not contribute in this process. Therefore, we include the two $\nu = 3$ terms in NC photon production, namely, the e_1 and c_1 couplings in Eq. (110). As mentioned in Sec. IIB2, there are many

other interaction terms at the same order as the e_1 and c_1 terms, *but these are the only two contributing in NC photon production*. Moreover, these two couplings are singled out in Ref. [67] as the low-energy manifestations of anomalous ρ and ω decay and are believed to give important contributions in coherent photon production from nuclei. Here we investigate the consequences of these two couplings. We emphasize that from the EFT perspective, the only way to determine these two couplings is by comparing the final theoretical result with data, rather than by calculating them from anomalous decay, which is not necessarily the only higher-energy physics contributing to these two operators. For example, as we discussed the off-shell couplings before, an off-shell coupling between N , π , and Δ can introduce the same matrix element as that induced by these two contact terms. Changing the off-shell couplings would also change these two contact terms to make the theory independent of the choice of off-shell couplings. Nevertheless, to perform concrete calculations with these two terms without precise information on the coupling strengths, we use the values from Ref. [67] in Figs. 16 and 17.

We can see the convergence of our calculations. The two couplings introduced in the ‘up to $\nu = 3$ ’ calculations increase the total cross section in both channels for both neutrino and antineutrino scattering, although the change is quite small. This constructive behavior is consistent with the results in Ref. [67]. However, as is easily seen, the contributions of this process are negligible in scattering off a single nucleon.

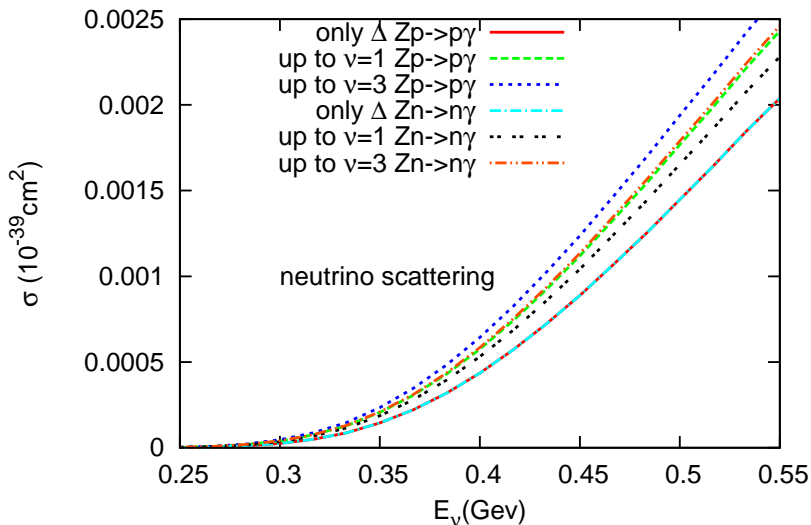


FIG. 16: Total cross section for NC photon production due to neutrino scattering. ‘Only Δ ’ indicates that only diagrams with Δ (both s and u channels) are included. ‘Up to $\nu = 1$ ’ includes all the diagrams at leading order. ‘Up to $\nu = 3$ ’ includes higher-order diagrams. The $\nu = 2$ terms are zero in these channels. The next-to-leading order in this channel is $\nu = 3$, whose couplings are from Ref. [67].

Naive power counting, however, does not give an accurate comparison between the Δ contributions and the N contributions at low energy. One reason is that the neutron does not have an electric charge at low energy, so its current should appear at higher order than the naive estimate. The second reason is that for the proton, due to the cancelation between the baryon current and the vector current, the neutral current is mainly composed of the axial-vector current, which reduces the strength of the neutral current. Because of these two

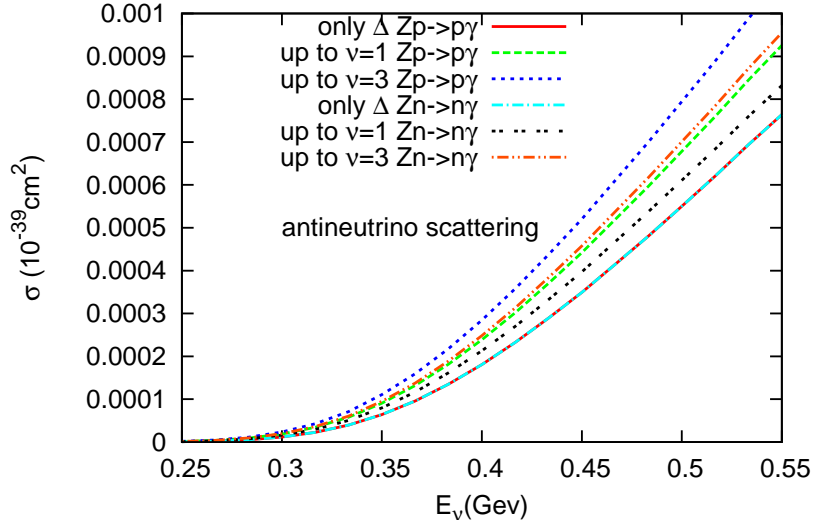


FIG. 17: Total cross section for NC photon productions due to antineutrino scattering. The curves are defined as in Fig. 16, and the channels are also indicated.

factors, the contributions of Δ and N are at the same scale far away from resonance, but near the resonance, the Δ dominates.

V. SUMMARY

Weak pion and photon production from nucleons and nuclei produce important backgrounds in neutrino-oscillation experiments and must therefore be understood quantitatively. In this work, we studied pion and photon neutrino production in a Lorentz-covariant, chirally invariant, meson-baryon EFT. For neutrino energies $E_\nu^{\text{Lab}} < 1 \text{ GeV}$, the resonant behavior of the Δ is important. We therefore included the Δ degrees of freedom explicitly in our EFT lagrangian, in a manner that is consistent with both Lorentz covariance and chiral symmetry.

It is well known that in a lagrangian with a finite number of interaction terms, including the Δ as a Rarita-Schwinger field leads to inconsistencies for strong couplings, strong fields, or large field variations. In a modern EFT with an infinite number of interaction terms, however, these pathologies can be removed, if we work at low energies with weak boson fields. This is because the problematic terms in the lagrangian produce local contact interactions that can be absorbed into other contact terms in the EFT lagrangian. Ambiguous, so-called off-shell couplings have also been shown to be redundant in the modern EFT framework. Thus the Δ resonance can be introduced into our EFT lagrangian in a consistent way. Moreover, we studied the structure of the dressed Δ propagator and found that it has a pole only in the spin-3/2 channel, so that we indeed have the correct number of resonant degrees of freedom.

Because of the symmetries built into our lagrangian, the vector currents are conserved and the axial-vector currents satisfy PCAC automatically, which is not true in some of the other approaches to this problem. Needless to say, a conserved vector current is crucial for computing photon production. By using vector and axial-vector transition currents that

were calibrated at high energies, we found results for pion production at lower energies that are consistent with the (limited) data. This was also true when vertices described by meson dominance were used. We also studied the convergence of our power-counting scheme at low energies and found that next-to-leading-order tree-level corrections are very small. Finally, we computed neutral-current photon production including contact interactions consistent with anomalous ρ and ω decays and found that, at least for a nucleon target, the resulting cross sections are unmeasurably small.

We are currently using this QHD/EFT framework to study the electroweak response of the nuclear many-body system, so that we can extend our results to pion and photon neutrino-production from nuclei, which are the true targets in existing neutrino-oscillation experiments.

Acknowledgments

This work was supported in part by the Department of Energy under Contract No. DE-FG02-87ER40365.

Appendix A: isospin indices, T matrices

Suppose \vec{t} are the generators of some (ir)reducible representation of $SU(2)$; then it is easy to prove that, in matrix form ($\tilde{\delta} \equiv -\underline{e}^{-i\pi t^y}$),

$$\tilde{\delta} \vec{t} \tilde{\delta}^{-1} = -\vec{t}^T, \quad (\text{A1})$$

where the superscript T denotes transpose. This equation justifies the use of $\tilde{\delta}$ as a metric linking the representation and the complex conjugate representation. One easily finds for $\mathcal{D}^{(3/2)}$, $\mathcal{D}^{(1)}$, and $\mathcal{D}^{(1/2)}$:

$$\tilde{\delta}^{ab} = \begin{pmatrix} 0 & 0 & 0 & 1 \\ 0 & 0 & -1 & 0 \\ 0 & 1 & 0 & 0 \\ -1 & 0 & 0 & 0 \end{pmatrix}, \quad \tilde{\delta}_{ab} = \begin{pmatrix} 0 & 0 & 0 & -1 \\ 0 & 0 & 1 & 0 \\ 0 & -1 & 0 & 0 \\ 1 & 0 & 0 & 0 \end{pmatrix}, \quad (\text{A2})$$

$$\tilde{\delta}^{ij} = \begin{pmatrix} 0 & 0 & -1 \\ 0 & 1 & 0 \\ -1 & 0 & 0 \end{pmatrix}, \quad \tilde{\delta}_{ij} = \begin{pmatrix} 0 & 0 & -1 \\ 0 & 1 & 0 \\ -1 & 0 & 0 \end{pmatrix}, \quad (\text{A3})$$

$$\tilde{\delta}^{AB} = \begin{pmatrix} 0 & 1 \\ -1 & 0 \end{pmatrix}, \quad \tilde{\delta}_{AB} = \begin{pmatrix} 0 & -1 \\ 1 & 0 \end{pmatrix}. \quad (\text{A4})$$

We turn now to the T matrices. As discussed in Sec. II A,

$$T_a^{\dagger iA} = \langle \frac{3}{2}; a | 1, \frac{1}{2}; i, A \rangle, \quad (\text{A5})$$

$$T_{iA}^a = \langle 1, \frac{1}{2}; i, A | \frac{3}{2}; a \rangle. \quad (\text{A6})$$

To be more specific:

$$T_a^\dagger +1A = \begin{pmatrix} 1 & 0 \\ 0 & \sqrt{\frac{1}{3}} \\ 0 & 0 \\ 0 & 0 \end{pmatrix}_{aA}, \quad T_a^\dagger 0A = \begin{pmatrix} 0 & 0 \\ \sqrt{\frac{2}{3}} & 0 \\ 0 & \sqrt{\frac{2}{3}} \\ 0 & 0 \end{pmatrix}_{aA}, \quad T_a^\dagger -1A = \begin{pmatrix} 0 & 0 \\ 0 & 0 \\ \sqrt{\frac{1}{3}} & 0 \\ 0 & 1 \end{pmatrix}_{aA}, \quad (\text{A7})$$

$$T_{+1A}^a = \begin{pmatrix} 1 & 0 & 0 & 0 \\ 0 & \sqrt{\frac{1}{3}} & 0 & 0 \end{pmatrix}_{Aa}, \quad T_{0A}^a = \begin{pmatrix} 0 & \sqrt{\frac{2}{3}} & 0 & 0 \\ 0 & 0 & \sqrt{\frac{2}{3}} & 0 \end{pmatrix}_{Aa}, \quad T_{-1A}^a = \begin{pmatrix} 0 & 0 & \sqrt{\frac{1}{3}} & 0 \\ 0 & 0 & 0 & 1 \end{pmatrix}_{Aa}. \quad (\text{A8})$$

It is easy to prove the following relations (here τ^i is a Pauli matrix):

$$\tau^i \tau_j = \tilde{\delta}_j^i + i \tilde{\epsilon}_{jk}^i \tau^k, \quad (\text{A9})$$

$$(P_i^j)_A^B \equiv T_{iA}^a T_a^\dagger jB = \tilde{\delta}_i^j \tilde{\delta}_A^B - \frac{1}{3} (\tau_i \tau^j)_A^B, \quad (\text{A10})$$

$$T_a^\dagger iA T_{iA}^b = \tilde{\delta}_a^b. \quad (\text{A11})$$

Here P_i^j is a projection operator that projects $\mathcal{H}(\frac{1}{2}) \otimes \mathcal{H}(1)$ onto $\mathcal{H}(\frac{3}{2})$.

A few words about $\tilde{\epsilon}_{jk}^i$ are in order here. We have the following transformations of pion fields:

$$\pi^i = u_I^i \pi^I \quad \text{here, } i = +1, 0, -1; \quad I = x, y, z; \quad (\text{A12})$$

$$\begin{pmatrix} \pi^{+1} \\ \pi^0 \\ \pi^{-1} \end{pmatrix} = \begin{pmatrix} \frac{-1}{\sqrt{2}} & \frac{-i}{\sqrt{2}} & 0 \\ 0 & 0 & 1 \\ \frac{1}{\sqrt{2}} & \frac{-i}{\sqrt{2}} & 0 \end{pmatrix} \begin{pmatrix} \pi^x \\ \pi^y \\ \pi^z \end{pmatrix}; \quad (\text{A13})$$

and hence we have

$$\begin{aligned} \pi \cdot \pi &= \pi^x \pi^x + \pi^y \pi^y + \pi^z \pi^z \\ &= -\pi^{+1} \pi^{-1} - \pi^{-1} \pi^{+1} + \pi^z \pi^z \\ &= \pi^{+1} \pi_{+1} + \pi^{-1} \pi_{-1} + \pi^0 \pi_0. \end{aligned} \quad (\text{A14})$$

Meanwhile, under such transformations,

$$\begin{aligned} \tilde{\epsilon}^{ijk} &\equiv u_I^i u_J^j u_K^k \epsilon^{IJK} = \det(\underline{u}_I^i) \epsilon^{ijk} = -i \epsilon^{ijk} \\ \implies \tilde{\epsilon}^{ijk} &= \begin{cases} -i, & \text{if } ijk = +1, 0, -1; \\ -i \delta_{\mathcal{P}}, & \text{if } ijk = \mathcal{P}(+1, 0, -1). \end{cases} \end{aligned} \quad (\text{A15})$$

Appendix B: C , P , and T symmetry realized in QCD

The symmetries C , P , and T are preserved in QCD. Based on the lagrangian in Eq. (5), we find the corresponding transformation rules shown in Table I. Inside the table, $\mathcal{P}_\nu^\mu = \text{diag}(1, -1, -1, -1)_{\mu\nu}$ and $\mathcal{T}_\nu^\mu = \text{diag}(-1, 1, 1, 1)_{\mu\nu}$.

	v^μ	$v_{(s)}^\mu$	a^μ	s	p	r^μ	l^μ	$f_{R\mu\nu}$	$f_{L\mu\nu}$	$f_{s\mu\nu}$
C	$-v^{T\mu}$	$-v_{(s)}^{T\mu}$	$a^{T\mu}$	s^T	p^T	$-l^{T\mu}$	$-r^{T\mu}$	$-f_{L\mu\nu}^T$	$-f_{R\mu\nu}^T$	$-f_{s\mu\nu}^T$
P	$\mathcal{P}_\nu^\mu v^\nu$	$\mathcal{P}_\nu^\mu v_{(s)}^\nu$	$-\mathcal{P}_\nu^\mu a^\nu$	s	$-p$	$\mathcal{P}_\nu^\mu l^\nu$	$\mathcal{P}_\nu^\mu r^\nu$	$\mathcal{P}_\mu^\lambda \mathcal{P}_\nu^\sigma f_{L\lambda\sigma}$	$\mathcal{P}_\mu^\lambda \mathcal{P}_\nu^\sigma f_{R\lambda\sigma}$	$\mathcal{P}_\mu^\lambda \mathcal{P}_\nu^\sigma f_{s\lambda\sigma}$
T	$-\mathcal{T}_\nu^\mu v^\nu$	$-\mathcal{T}_\nu^\mu v_{(s)}^\nu$	$-\mathcal{T}_\nu^\mu a^\nu$	s	$-p$	$-\mathcal{T}_\nu^\mu l^\nu$	$-\mathcal{T}_\nu^\mu r^\nu$	$-\mathcal{T}_\mu^\lambda \mathcal{T}_\nu^\sigma f_{L\lambda\sigma}$	$-\mathcal{T}_\mu^\lambda \mathcal{T}_\nu^\sigma f_{R\lambda\sigma}$	$-\mathcal{T}_\mu^\lambda \mathcal{T}_\nu^\sigma f_{s\lambda\sigma}$

TABLE I: Transformations of background fields under C , P , and T operations. The transformed spacetime arguments are not shown here.

Appendix C: C , P , and T symmetry realized in QHD

The C , P , and T transformation rules are summarized in Table II. A plus sign means normal, while a minus sign means abnormal, i.e., an extra minus sign exists in the transformation. The convention for Dirac matrices sandwiched by nucleon and/or Δ fields are

$$C\bar{N}\Gamma NC^{-1} = \begin{cases} -N^T \Gamma^T \bar{N}^T, & \text{normal;} \\ N^T \Gamma^T \bar{N}^T, & \text{abnormal.} \end{cases} \quad (C1)$$

$$C(\bar{\Delta}\Gamma N + \bar{N}\Gamma\Delta)C^{-1} = \begin{cases} -\Delta^T \Gamma^T \bar{N}^T - N^T \Gamma^T \bar{\Delta}^T, & \text{normal;} \\ +\Delta^T \Gamma^T \bar{N}^T + N^T \Gamma^T \bar{\Delta}^T, & \text{abnormal.} \end{cases} \quad (C2)$$

$$Ci(\bar{\Delta}\Gamma N - \bar{N}\Gamma\Delta)C^{-1} = \begin{cases} +i\Delta^T \Gamma^T \bar{N}^T - iN^T \Gamma^T \bar{\Delta}^T, & \text{normal;} \\ -i\Delta^T \Gamma^T \bar{N}^T + iN^T \Gamma^T \bar{\Delta}^T, & \text{abnormal.} \end{cases} \quad (C3)$$

Here, in Eqs. (C1), (C2), and (C3), the extra minus sign arises because the fermion fields anticommute. The factor of i in Eq. (C3) is due to the requirement of hermiticity of the lagrangian. To make the analysis easier for $\bar{\Delta}\Gamma N + C.C.$, we can just attribute a minus sign to an i under the C transformation. Whenever an i exists, the lagrangian takes the form $i(\bar{\Delta}\Gamma N - \bar{N}\Gamma\Delta)$. When no i exists, the lagrangian will be like $\bar{\Delta}\Gamma N + \bar{N}\Gamma\Delta$.

For P and T transformations, the conventions are the same for N and Δ fields, except for an extra minus sign in the parity assignment for each Δ field [69], so we list only the N case (\mathcal{P}_ν^μ and \mathcal{T}_ν^μ can be found in Appendix B):

$$P\bar{N}\Gamma_\mu NP^{-1} = \begin{cases} \bar{N}\mathcal{P}_\mu^\nu \Gamma_\nu N, & \text{normal;} \\ -\bar{N}\mathcal{P}_\mu^\nu \Gamma_\nu N, & \text{abnormal.} \end{cases} \quad (C4)$$

$$T\bar{N}\Gamma_\mu NT^{-1} = \begin{cases} \bar{N}\mathcal{T}_\mu^\nu \Gamma_\nu N, & \text{normal;} \\ -\bar{N}\mathcal{T}_\mu^\nu \Gamma_\nu N, & \text{abnormal.} \end{cases} \quad (C5)$$

It is easy to generalize these results to $\Gamma_{\mu\nu}$, etc.

Suppose an isovector object is denoted as $O_\mu \equiv O_{i\mu}t^i$, then the conventions are explained

	γ^μ	$\sigma^{\mu\nu}$	1	$\gamma^\mu\gamma^5$	$i\gamma^5$	i	$i\overleftrightarrow{\partial}$	$\epsilon^{\mu\nu\alpha\beta}$	\tilde{a}_μ	\tilde{v}_μ	$\tilde{v}_{\mu\nu}$	ρ_μ	$\rho_{\mu\nu}$	$\bar{\rho}_{\mu\nu}$	V_μ	$V_{\mu\nu}$	$\bar{V}_{\mu\nu}$	$F_{\mu\nu}^{(\pm)}$	$f_{s\mu\nu}$	$\bar{F}_{\mu\nu}^{(\pm)}$	$\bar{f}_{s\mu\nu}$
C	-	-	+	+	+	-	-	+	+	-	-	-	-	-	-	-	-	\mp	-	\mp	-
P	+	+	+	-	-	+	+	-	-	+	+	+	+	-	+	+	-	\pm	+	\mp	-
T	-	-	+	-	-	-	-	-	-	-	-	-	-	+	-	-	+	-	-	+	+

TABLE II: Transformation properties of objects under C , P , and T .

below:

$$CO_\mu C^{-1} = \begin{cases} O_\mu^T, & \text{normal;} \\ -O_\mu^T, & \text{abnormal.} \end{cases} \quad (\text{C6})$$

$$PO_\mu P^{-1} = \begin{cases} \mathcal{P}_\mu^\nu O_\nu, & \text{normal;} \\ -\mathcal{P}_\mu^\nu O_\nu, & \text{abnormal.} \end{cases} \quad (\text{C7})$$

$$TO_\mu T^{-1} = \begin{cases} \mathcal{T}_\mu^\nu O_\nu, & \text{normal;} \\ -\mathcal{T}_\mu^\nu O_\nu, & \text{abnormal.} \end{cases} \quad (\text{C8})$$

The same convention applies to the isovector (pseudo)tensors. For isovector (pseudo)scalars, the \mathcal{P} and \mathcal{T} should be changed to $\mathbf{1}$. For the C transformation, O^T means transposing both isospin and Dirac matrices in the definition of O , if necessary.

Appendix D: Form factors for currents

Here we use matrix elements of the various currents to define the form factors produced by the EFT lagrangian [5]. Note that q^μ is defined as the *incoming* momentum transfer at the vertex; in terms of initial and final nucleon momenta, $q^\mu \equiv p_{nf}^\mu - p_{ni}^\mu$. When a pion is emitted, $p_{ni}^\mu + q^\mu = p_{nf}^\mu + k_\pi^\mu$.

To derive these expressions, it is necessary to expand terms in the lagrangian to leading

order in pion and external fields. Useful results are given below:

$$\text{Tr}\left(\frac{\tau^i}{2}[U, \partial^\mu U^\dagger]\right) \approx 2i\epsilon^{ijk} \frac{\pi_j}{f_\pi} \frac{\partial_\mu \pi_k}{f_\pi}, \quad (\text{D1})$$

$$\text{Tr}\left(\frac{\tau^i}{2}\{U, \partial^\mu U^\dagger\}\right) \approx -2i \frac{\partial_\mu \pi^i}{f_\pi}, \quad (\text{D2})$$

$$\xi^\dagger \frac{\tau^i}{2} \xi + \xi \frac{\tau^i}{2} \xi^\dagger \approx \tau^i, \quad (\text{D3})$$

$$\xi^\dagger \frac{\tau^i}{2} \xi - \xi \frac{\tau^i}{2} \xi^\dagger \approx -\epsilon^{ijk} \frac{\pi_j}{f_\pi} \tau_k, \quad (\text{D4})$$

$$\xi^\dagger \frac{\tau^i}{2} \xi \approx \frac{\tau^i}{2} - \epsilon^{ijk} \frac{\pi_j}{f_\pi} \frac{\tau_k}{2}, \quad (\text{D5})$$

$$\xi \frac{\tau^i}{2} \xi^\dagger \approx \frac{\tau^i}{2} + \epsilon^{ijk} \frac{\pi_j}{f_\pi} \frac{\tau_k}{2}, \quad (\text{D6})$$

$$\tilde{v}_\mu \approx \frac{1}{2f_\pi^2} \epsilon^{ijk} \pi_j \partial_\mu \pi_k \frac{\tau_i}{2} - \mathbf{v}_{i\mu} \frac{\tau^i}{2} - \epsilon^{ijk} \frac{\pi_j}{f_\pi} \frac{\tau_k}{2} \mathbf{a}_{i\mu}, \quad (\text{D7})$$

$$\tilde{a}_\mu \approx \frac{1}{f_\pi} \partial_\mu \pi^i \frac{\tau_i}{2} + \mathbf{a}_{i\mu} \frac{\tau^i}{2} + \epsilon^{ijk} \frac{\pi_j}{f_\pi} \frac{\tau_k}{2} \mathbf{v}_{i\mu}, \quad (\text{D8})$$

$$\begin{aligned} \tilde{v}_{\mu\nu} \approx & \frac{1}{f_\pi^2} \epsilon^{ijk} \partial_\mu \pi_j \partial_\nu \pi_k \frac{\tau_i}{2} - \left(i \left[\frac{1}{f_\pi} \partial_\mu \pi^i \frac{\tau_i}{2}, \mathbf{a}_\nu + \epsilon^{ijk} \frac{\pi_j}{f_\pi} \frac{\tau_k}{2} \mathbf{v}_{i\nu} \right] - (\mu \leftrightarrow \nu) \right) \\ & + \text{background interference terms,} \end{aligned} \quad (\text{D9})$$

$$\rho_{\mu\nu} = \partial_{[\mu} \rho_{\nu]} + i\bar{g}_\rho [\rho_\mu, \rho_\nu] + i([\tilde{v}_\mu, \rho_\nu] - \mu \leftrightarrow \nu), \quad (\text{D10})$$

$$f_{L\mu\nu} + f_{R\mu\nu} = 2\partial_{[\mu} \mathbf{v}_{\nu]} - 2i[\mathbf{v}_\mu, \mathbf{v}_\nu] - 2i[\mathbf{a}_\mu, \mathbf{a}_\nu], \quad (\text{D11})$$

$$f_{L\mu\nu} - f_{R\mu\nu} = -2\partial_{[\mu} \mathbf{a}_{\nu]} + 2i[\mathbf{v}_\mu, \mathbf{a}_\nu] + 2i[\mathbf{a}_\mu, \mathbf{v}_\nu], \quad (\text{D12})$$

$$\begin{aligned} F_{\mu\nu}^{(+)} &= \xi^\dagger \frac{\tau^i}{2} \xi f_{Li\mu\nu} + \xi \frac{\tau^i}{2} \xi^\dagger f_{Ri\mu\nu} \\ &= \frac{\tau^i}{2} (f_{Li\mu\nu} + f_{Ri\mu\nu}) - \epsilon^{ijk} \frac{\pi_j}{f_\pi} \tau_k (f_{Li\mu\nu} - f_{Ri\mu\nu}) \\ &\approx 2\partial_{[\mu} \mathbf{v}_{\nu]} + 2\epsilon^{ijk} \frac{\pi_j}{f_\pi} \frac{\tau_k}{2} \partial_{[\mu} \mathbf{a}_{i\nu]} + \text{background interference,} \end{aligned} \quad (\text{D13})$$

$$\begin{aligned} F_{\mu\nu}^{(-)} &= \xi^\dagger \frac{\tau^i}{2} \xi f_{Li\mu\nu} - \xi \frac{\tau^i}{2} \xi^\dagger f_{Ri\mu\nu} \\ &= \frac{\tau^i}{2} (f_{Li\mu\nu} - f_{Ri\mu\nu}) - \epsilon^{ijk} \frac{\pi_j}{f_\pi} \tau_k (f_{Li\mu\nu} + f_{Ri\mu\nu}) \\ &\approx -2\partial_{[\mu} \mathbf{a}_{\nu]} - 2\epsilon^{ijk} \frac{\pi_j}{f_\pi} \frac{\tau_k}{2} \partial_{[\mu} \mathbf{v}_{i\nu]} + \text{background interference.} \end{aligned} \quad (\text{D14})$$

We now proceed to determine the matrix elements.

$$\begin{aligned}
\langle N, B | V_\mu^i | N, A \rangle &= \left[\bar{u}_f \gamma_\mu u_i + \frac{\beta^{(1)}}{M^2} \bar{u}_f (q^2 \gamma_\mu - \not{q} q_\mu) u_i \right. \\
&\quad \left. - \frac{g_\rho}{g_\gamma} \frac{q^2 g_{\mu\nu} - q_\mu q_\nu}{q^2 - m_\rho^2} \bar{u}_f \gamma^\nu u_i \right] \langle B | \frac{\tau^i}{2} | A \rangle \\
&\quad + \left[2\lambda^{(1)} \bar{u}_f \frac{\sigma_{\mu\nu} i q^\nu}{2M} u_i - \frac{f_\rho g_\rho}{g_\gamma} \frac{q^2}{q^2 - m_\rho^2} \bar{u}_f \frac{\sigma_{\mu\nu} i q^\nu}{2M} u_i \right] \langle B | \frac{\tau^i}{2} | A \rangle \\
&\equiv \langle B | \frac{\tau^i}{2} | A \rangle \bar{u}_f \left(\gamma_\mu + 2\delta F_1^{V,md} \frac{q^2 \gamma_\mu - \not{q} q_\mu}{q^2} + 2F_2^{V,md} \frac{\sigma_{\mu\nu} i q^\nu}{2M} \right) u_i
\end{aligned} \tag{D15}$$

$$\equiv \langle B | \frac{\tau^i}{2} | A \rangle \bar{u}_f \Gamma_{V\mu}(q) u_i \tag{D16}$$

$$\stackrel{\text{on shell}}{\equiv} \langle B | \frac{\tau^i}{2} | A \rangle \bar{u}_f \left(2F_1^{V,md} \gamma_\mu + 2F_2^{V,md} \frac{\sigma_{\mu\nu} i q^\nu}{2M} \right) u_i, \tag{D17}$$

$$\begin{aligned}
\langle N, B | J_\mu^B | N, A \rangle &= \left[\bar{u}_f \gamma_\mu u_i + \frac{\beta^{(0)}}{M^2} \bar{u}_f (q^2 \gamma_\mu - \not{q} q_\mu) u_i \right. \\
&\quad \left. - \frac{2g_v}{3g_\gamma} \frac{q^2 g_{\mu\nu} - q_\mu q_\nu}{q^2 - m_v^2} \bar{u}_f \gamma^\nu u_i \right] \delta_B^A \\
&\quad + \left[2\lambda^{(0)} \bar{u}_f \frac{\sigma_{\mu\nu} i q^\nu}{2M} u_i - \frac{2f_v g_v}{3g_\gamma} \frac{q^2}{q^2 - m_v^2} \bar{u}_f \frac{\sigma_{\mu\nu} i q^\nu}{2M} u_i \right] \delta_B^A \\
&\equiv \delta_B^A \bar{u}_f \left(\gamma_\mu + 2\delta F_1^{S,md} \frac{q^2 \gamma_\mu - \not{q} q_\mu}{q^2} + 2F_2^{S,md} \frac{\sigma_{\mu\nu} i q^\nu}{2M} \right) u_i
\end{aligned} \tag{D18}$$

$$\equiv \delta_B^A \bar{u}_f \Gamma_{B\mu}(q) u_i \tag{D19}$$

$$\stackrel{\text{on shell}}{\equiv} \delta_B^A \bar{u}_f \left(2F_1^{S,md} \gamma_\mu + 2F_2^{S,md} \frac{\sigma_{\mu\nu} i q^\nu}{2M} \right) u_i, \tag{D20}$$

$$\begin{aligned}
& \langle N, B; \pi, j, k_\pi | A_\mu^i | N, A \rangle \\
&= -\frac{\epsilon^i{}_{jk}}{f_\pi} \langle B | \frac{\tau^k}{2} | A \rangle \bar{u}_f \gamma^\nu u_i \left[g_{\mu\nu} + \frac{\beta^{(1)}}{M^2} (q \cdot (q - k_\pi) g_{\mu\nu} - (q - k_\pi)_\mu q_\nu) \right. \\
&\quad \left. - \frac{g_\rho}{g_\gamma} \frac{q \cdot (q - k_\pi) g_{\mu\nu} - (q - k_\pi)_\mu q_\nu}{(q - k_\pi)^2 - m_\rho^2} \right] \\
&\quad - \frac{\epsilon^i{}_{jk}}{f_\pi} \langle B | \frac{\tau^k}{2} | A \rangle \bar{u}_f \frac{\sigma_{\mu\nu} i q^\nu}{2M} u_i \left[2\lambda^{(1)} - \frac{f_\rho g_\rho}{g_\gamma} \frac{q \cdot (q - k_\pi)}{(q - k_\pi)^2 - m_\rho^2} \right] \tag{D21}
\end{aligned}$$

$$\begin{aligned}
&\equiv -\frac{\epsilon^i{}_{jk}}{f_\pi} \langle B | \frac{\tau^k}{2} | A \rangle \bar{u}_f \gamma^\nu u_i \\
&\quad \times \left[g_{\mu\nu} + 2\delta F_1^{V,md} ((q - k_\pi)^2) \frac{q \cdot (q - k_\pi) g_{\mu\nu} - (q - k_\pi)_\mu q_\nu}{(q - k_\pi)^2} \right] \\
&\quad - \frac{\epsilon^i{}_{jk}}{f_\pi} \langle B | \frac{\tau^k}{2} | A \rangle \bar{u}_f \frac{\sigma_{\mu\nu} i q^\nu}{2M} u_i \left[2\lambda^{(1)} + 2\delta F_2^{V,md} ((q - k_\pi)^2) \frac{q \cdot (q - k_\pi)}{(q - k_\pi)^2} \right] \tag{D22}
\end{aligned}$$

$$\equiv \frac{\epsilon^i{}_{jk}}{f_\pi} \langle B | \frac{\tau^k}{2} | A \rangle \bar{u}_f \Gamma_{A\pi\mu}(q, k_\pi) u_i . \tag{D23}$$

Now we consider $\langle N, B | A_\mu^i | N, A \rangle$ and $\langle N, B; \pi, j | V_\mu^i | N, A \rangle$. In the *chiral limit*, we find

$$\begin{aligned}
\langle N, B | A_\mu^i | N, A \rangle &= -\langle B | \frac{\tau^i}{2} | A \rangle \bar{u}_f \gamma^\nu \gamma^5 u_i \left[g_A \left(g_{\mu\nu} - \frac{q_\mu q_\nu}{q^2} \right) - \frac{\beta_A^{(1)}}{M^2} (q^2 g_{\mu\nu} - q_\mu q_\nu) \right. \\
&\quad \left. - 2c_{a_1} g_{a_1} \frac{q^2 g_{\mu\nu} - q_\mu q_\nu}{q^2 - m_{a_1}^2} \right] , \tag{D24}
\end{aligned}$$

$$\begin{aligned}
&\langle N, B; \pi, j, k_\pi | V_\mu^i | N, A \rangle \\
&= \frac{\epsilon^i{}_{jk}}{f_\pi} \langle B | \frac{\tau^k}{2} | A \rangle \bar{u}_f \gamma^\nu \gamma^5 u_i \left[g_A g_{\mu\nu} - \frac{\beta_A^{(1)}}{M^2} [q \cdot (q - k_\pi) g_{\mu\nu} - (q - k_\pi)_\mu q_\nu] \right. \\
&\quad \left. - 2c_{a_1} g_{a_1} \frac{q \cdot (q - k_\pi) g_{\mu\nu} - (q - k_\pi)_\mu q_\nu}{(q - k_\pi)^2 - m_{a_1}^2} \right] . \tag{D25}
\end{aligned}$$

Now suppose there is only one manifestly chiral-symmetry-breaking term, i.e., the mass term for pions; then the pion-pole contribution associated with the g_A coupling in $\langle N, B | A_\mu^i | N, A \rangle$ will become $g_A [g_{\mu\nu} - q_\mu q_\nu / (q^2 - m_\pi^2)]$, while the other parts in $\langle N, B | A_\mu^i | N, A \rangle$, as well as the whole $\langle N, B; \pi, j | V_\mu^i | N, A \rangle$, will remain unchanged. However, we must realize that there are other possible chiral-symmetry-breaking terms contributing to $\langle N, B | A_\mu^i | N, A \rangle$. For example, $(m_\pi^2/M) \bar{N} i \gamma^5 (U - U^\dagger) N$ will contribute to $\langle N, B | A_\mu^i | N, A \rangle$ as

$$-\frac{2m_\pi^2}{M^2} \frac{q_\mu \not{q} \gamma^5}{q^2 - m_\pi^2} \langle B | \frac{\tau^i}{2} | A \rangle .$$

To simplify the fitting procedures, we will use the following form factors:

$$\langle N, B | A_\mu^i | N, A \rangle = -G_A^{md}(q^2) \langle B | \frac{\tau^i}{2} | A \rangle \bar{u}_f \left(g_{\mu\nu} - \frac{q_\mu q_\nu}{q^2 - m_\pi^2} \right) \gamma^\nu \gamma^5 u_i, \quad (\text{D26})$$

$$\begin{aligned} \langle N, B; \pi, j, k_\pi | V_\mu^i | N, A \rangle &= \frac{\epsilon_{jk}^i}{f_\pi} \langle B | \frac{\tau^k}{2} | A \rangle \bar{u}_f \gamma^\nu \gamma^5 u_i \left[g_A g_{\mu\nu} \right. \\ &\quad \left. + \delta G_A^{md}((q - k_\pi)^2) \frac{q \cdot (q - k_\pi) g_{\mu\nu} - (q - k_\pi)_\mu q_\nu}{(q - k_\pi)^2} \right]. \end{aligned} \quad (\text{D27})$$

The required definitions can be found in Eqs. (43) and (44).

Finally, we calculate the pion form factor $\langle \pi, k | V_\mu^i | \pi, j \rangle$:

$$\begin{aligned} \langle \pi, k, k_\pi | V_\mu^i | \pi, j, k_\pi - q \rangle &= i \epsilon_k^{ij} (2k_\pi - q)_\mu \\ &\quad + 2i \frac{g_{\rho\pi\pi}}{g_\gamma} \epsilon_k^{ij} \frac{q^2}{m_\rho^2} \frac{1}{q^2 - m_\rho^2} (q \cdot k_\pi q_\mu - q^2 k_{\pi\mu}) \\ q^2 \rightarrow m_\rho^2 \text{ in numerator} &\longrightarrow i \epsilon_k^{ij} (2k_\pi - q)_\mu \\ &\quad + 2i \frac{g_{\rho\pi\pi}}{g_\gamma} \epsilon_k^{ij} \frac{1}{q^2 - m_\rho^2} (q \cdot k_\pi q_\mu - q^2 k_{\pi\mu}) \end{aligned} \quad (\text{D28})$$

$$\begin{aligned} \text{pion on shell} &= i \epsilon_k^{ij} (2k_\pi - q)_\mu \left(1 - \frac{g_{\rho\pi\pi}}{g_\gamma} \frac{q^2}{q^2 - m_\rho^2} \right) \\ &\equiv i \epsilon_k^{ij} (2k_\pi - q)_\mu F_\pi^{md}(q^2) \end{aligned} \quad (\text{D29})$$

$$\begin{aligned} &\implies \\ \langle \pi, k, k_\pi | V_\mu^i | \pi, j, k_\pi - q \rangle &= i \epsilon_k^{ij} \left[(2k_\pi - q)_\mu + 2\delta F_\pi^{md}(q^2) \left(k_{\pi\mu} - \frac{q \cdot k_\pi}{q^2} q_\mu \right) \right] \\ &\equiv i \epsilon_k^{ij} P_{V\mu}(q, k_\pi). \end{aligned} \quad (\text{D30})$$

$$\text{Here,} \quad \delta F_\pi^{md}(q^2) = F_\pi^{md}(q^2) - F_\pi^{md}(0). \quad (\text{D31})$$

Appendix E: Free Δ propagator and self-energy insertion

Normally, the free, spin-3/2 field's propagator can be decomposed as [45, 70, 71]

$$S_F^{0\mu\nu}(p) \equiv -\frac{1}{\not{p} - m + i\epsilon} P^{(\frac{3}{2})\mu\nu} - \frac{1}{\sqrt{3}m} P_{12}^{(\frac{1}{2})\mu\nu} - \frac{1}{\sqrt{3}m} P_{21}^{(\frac{1}{2})\mu\nu} + \frac{2}{3m^2} (\not{p} + m) P_{22}^{(\frac{1}{2})\mu\nu} , \quad (\text{E1})$$

$$P^{(\frac{3}{2})\mu\nu} = g^{\mu\nu} - \frac{1}{3} \gamma^\mu \gamma^\nu + \frac{1}{3p^2} \gamma^{[\mu} p^{\nu]} \not{p} - \frac{2}{3p^2} p^\mu p^\nu , \quad (\text{E2})$$

$$P_{11}^{(\frac{1}{2})\mu\nu} = \frac{1}{3} \gamma^\mu \gamma^\nu - \frac{1}{3p^2} \gamma^{[\mu} p^{\nu]} \not{p} - \frac{1}{3p^2} p^\mu p^\nu , \quad (\text{E3})$$

$$P_{12}^{(\frac{1}{2})\mu\nu} = \frac{1}{\sqrt{3}p^2} (-p^\mu p^\nu + \gamma^\mu p^\nu \not{p}) , \quad (\text{E4})$$

$$P_{21}^{(\frac{1}{2})\mu\nu} = \frac{1}{\sqrt{3}p^2} (p^\mu p^\nu - \gamma^\nu p^\mu \not{p}) , \quad (\text{E5})$$

$$P_{22}^{(\frac{1}{2})\mu\nu} = \frac{1}{p^2} p^\mu p^\nu . \quad (\text{E6})$$

It is easy to prove the following relations:

$$(P_{ij}^{(I)})^{\mu\nu} (P_{kl}^{(J)})_{\nu\lambda} = \delta_{IJ} \delta_{jk} (P_{il}^{(I)})_\lambda^\mu , \quad (\text{E7})$$

$$\gamma^\mu P_{\mu\nu}^{(\frac{3}{2})} = P_{\mu\nu}^{(\frac{3}{2})} \gamma^\nu = 0 , \quad (\text{E8})$$

$$p^\mu P_{\mu\nu}^{(\frac{3}{2})} = P_{\mu\nu}^{(\frac{3}{2})} p^\nu = 0 , \quad (\text{E9})$$

$$P^{(\frac{3}{2})} + P_{11}^{(\frac{1}{2})} + P_{22}^{(\frac{1}{2})} = \mathbf{1} , \quad (\text{E10})$$

$$P_{11}^{(\frac{1}{2})} + P_{22}^{(\frac{1}{2})} \equiv P^{(\frac{3}{2}\perp)} , \quad (\text{E11})$$

$$\left[P^{(\frac{3}{2})} , \not{p} \right] = 0 , \quad (\text{E12})$$

$$\left[P_{11}^{(\frac{1}{2})} , \not{p} \right] = 0 , \quad (\text{E13})$$

$$\left[P_{22}^{(\frac{1}{2})} , \not{p} \right] = 0 . \quad (\text{E14})$$

With the preceding properties of the projection operators, we easily find

$$\begin{aligned}
S_F^0(p) &= P^{(\frac{3}{2})} \frac{-1}{\not{p} - m + i\epsilon} P^{(\frac{3}{2})} - \frac{1}{\sqrt{3}m} P_{12}^{(\frac{1}{2})} - \frac{1}{\sqrt{3}m} P_{21}^{(\frac{1}{2})} + P_{22}^{(\frac{1}{2})} \frac{2}{3m^2} (\not{p} + m) P_{22}^{(\frac{1}{2})} \\
&= P^{(\frac{3}{2})} \frac{-1}{\not{p} - m + i\epsilon} P^{(\frac{3}{2})} \\
&\quad + P^{(\frac{3}{2}\perp)} \left[-\frac{1}{\sqrt{3}m} P_{12}^{(\frac{1}{2})} - \frac{1}{\sqrt{3}m} P_{21}^{(\frac{1}{2})} + P_{22}^{(\frac{1}{2})} \frac{2}{3m^2} (\not{p} + m) P_{22}^{(\frac{1}{2})} \right] P^{(\frac{3}{2}\perp)} \quad (\text{E15})
\end{aligned}$$

$$\equiv S_F^{0(\frac{3}{2})}(p) + S_F^{0(\frac{3}{2}\perp)}(p) . \quad (\text{E16})$$

Following the analysis in Ref. [45], the self-energy of the Δ can be defined as $\Sigma_{\mu\nu} \equiv \Sigma^\Delta g_{\mu\nu} + \delta\Sigma_{\mu\nu}$. It follows that in $\delta\Sigma_{\mu\nu}$, the indices can only have structures like the products $(\gamma_\mu, p_\mu)(\gamma_\nu, p_\nu)$. Then we find quite an interesting property of Σ (the $\mu\nu$ indices are suppressed):

$$\begin{aligned}
\Sigma &= \Sigma^\Delta g + \delta\Sigma \\
&= (P^{(\frac{3}{2})} + P^{(\frac{3}{2}\perp)})(\Sigma^\Delta g + \delta\Sigma)(P^{(\frac{3}{2})} + P^{(\frac{3}{2}\perp)}) \\
&= P^{(\frac{3}{2})}\Sigma^\Delta g P^{(\frac{3}{2})} + P^{(\frac{3}{2}\perp)}\Sigma P^{(\frac{3}{2}\perp)} \\
&\quad + P^{(\frac{3}{2})}(\Sigma^\Delta g + \delta\Sigma)P^{(\frac{3}{2}\perp)} + P^{(\frac{3}{2}\perp)}(\Sigma^\Delta g + \delta\Sigma)P^{(\frac{3}{2})} \\
&= P^{(\frac{3}{2})}\Sigma^\Delta P^{(\frac{3}{2})} + P^{(\frac{3}{2}\perp)}\Sigma P^{(\frac{3}{2}\perp)} \\
&\equiv \Sigma^{(\frac{3}{2})} + \Sigma^{(\frac{3}{2}\perp)} . \quad (\text{E17})
\end{aligned}$$

In the proof, we make use of $[P^{(\frac{3}{2})}, \Sigma^\Delta] = 0$ and $[P^{(\frac{3}{2}\perp)}, \Sigma^\Delta] = 0$, since the only possible spin structures of Σ^Δ are $\mathbf{1}$, \not{p} , and γ^5 (parity violation), which commute with the two projection operators. This implies $P^{(\frac{3}{2})}\Sigma^\Delta g P^{(\frac{3}{2}\perp)} = 0$ and $P^{(\frac{3}{2}\perp)}\Sigma^\Delta g P^{(\frac{3}{2})} = 0$. We also make use of Eqs. (E8) and (E9), so we get $P^{(\frac{3}{2})}\delta\Sigma P^{(\frac{3}{2}\perp)} = 0$ and $P^{(\frac{3}{2}\perp)}\delta\Sigma P^{(\frac{3}{2})} = 0$.

Appendix F: Construction of a Delta interaction term

We show an example of constructing a term in the lagrangian with interactions between pions and the Δ . Consider

$$\frac{-i}{2} \bar{\Delta}_\mu^a \{ \sigma^{\mu\nu}, \tilde{\mathcal{A}}_a^b \gamma^5 \} \Delta_{b\nu} .$$

It can be shown that

$$\begin{aligned}
&\frac{-i}{2} \bar{\Delta}_\mu^a \{ \sigma^{\mu\nu}, \tilde{\mathcal{A}}_a^b \gamma^5 \} \Delta_{b\nu} \\
&= \bar{\Delta}^{a\mu} \tilde{\mathcal{A}}_a^b \gamma^5 \Delta_{b\mu} + \bar{\Delta}_\mu^a [-\gamma^\mu \tilde{a}^\nu \gamma^5 - \gamma^\nu \tilde{a}^\mu \gamma^5 + \gamma^\mu \tilde{\mathcal{A}} \gamma^\nu \gamma^5]_a^b \Delta_{b\nu} . \quad (\text{F1})
\end{aligned}$$

According to the argument in Sec. II C 3, the original coupling and $\bar{\Delta}^{a\mu} \tilde{\mathcal{A}}_a^b \gamma^5 \Delta_{b\mu}$ are equivalent in low-energy effective theory. We use the second form in our lagrangian.

Appendix G: kinematics

Following a standard calculation, we find the total cross section:

$$\begin{aligned}
\sigma &= \int \frac{|\overline{M}|^2}{4|p_{li}^L \cdot p_{ni}^L|} (2\pi)^4 \delta^{(4)} \left(\sum_i p_i^L \right) \frac{d^3 \vec{p}_{lf}^L}{(2\pi)^3 2E_{lf}^L} \frac{d^3 \vec{p}_\pi^L}{(2\pi)^3 2E_\pi^L} \frac{d^3 \vec{p}_{nf}^L}{(2\pi)^3 2E_{nf}^L} \\
&= \int \frac{|\overline{M}|^2}{4|p_{li}^L \cdot p_{ni}^L|} (2\pi)^4 \delta^{(4)}(q + p_{ni} - p_{nf} - p_\pi) \frac{d^3 \vec{p}_{lf}^L}{(2\pi)^3 2E_{lf}^L} \frac{d^3 \vec{p}_\pi^L}{(2\pi)^3 2E_\pi^L} \frac{d^3 \vec{p}_{nf}^L}{(2\pi)^3 2E_{nf}^L} \\
&= \int \frac{|\overline{M}|^2}{4|p_{li}^L \cdot p_{ni}^L|} (2\pi)^4 \delta(q^0 + p_{ni}^0 - p_{nf}^0 - p_\pi^0) \frac{1}{(2\pi)^3 2E_{nf}} \frac{d^3 \vec{p}_{lf}^L}{(2\pi)^3 2E_{lf}^L} \frac{d^3 \vec{p}_\pi^L}{(2\pi)^3 2E_\pi^L} \\
&= \int \frac{|\overline{M}|^2}{32M_n} \frac{1}{(2\pi)^5} \frac{|\vec{p}_\pi|}{E_\pi + E_{nf}} \frac{|\vec{p}_{lf}^L|}{|\vec{p}_{li}^L|} d\Omega_\pi dE_{lf}^L d\Omega_{lf}^L . \tag{G1}
\end{aligned}$$

It is quite complicated to calculate the boundary of phase space in terms of the integration variables in the preceding equations. Later, we will work out the boundary of phase space in terms of the invariant variables Q^2 and $M_{\pi n}$ in the cm frame of the whole system, so we would like to have the following:

$$Q^2 = -M_{lf}^2 + 2E_{li}^L(E_{lf}^L - |\vec{p}_{lf}^L| \cos \theta_{lf}^L) , \tag{G2}$$

$$M_{\pi n}^2 = (q^L + p_{ni}^L)^2 = -Q^2 + M_n^2 + 2M_n(E_{li}^L - E_{lf}^L) , \tag{G3}$$

from which it follows

$$dQ^2 dM_{\pi n}^2 = 4M_n E_{li}^L |\vec{p}_{lf}^L| dE_{lf}^L d\cos \theta_{lf}^L . \tag{G4}$$

By using the invariance of the cross section with respect to rotations around the incoming lepton direction, we have $\int d\Omega_{lf}^L = \int d\cos \theta_{lf}^L 2\pi$, and thus

$$\sigma = \int \frac{|\overline{M}|^2}{64M_n^2} \frac{1}{(2\pi)^5} \frac{|\vec{p}_\pi|}{E_\pi + E_{nf}} \frac{\pi}{|\vec{p}_{li}^L| E_{li}^L} d\Omega_\pi dM_{\pi n}^2 dQ^2 . \tag{G5}$$

In the isobaric frame, there is no preference in the direction of the outgoing pion. Thus the boundary of Ω_π is the whole solid angle in the isobaric frame. Now let's work out the boundary of phase space in the cm frame. We have

$$M_A^2 \equiv p_A^2 = (p_{ni}^L + p_{li}^L)^2 = (M_n + E_{li}^L)^2 - (E_{li}^L)^2 = M_n^2 + 2M_n E_{li}^L , \tag{G6}$$

$$M_{\pi n}^2 \equiv (p_\pi + p_{nf})^2 = (p_A^C - p_{lf}^C)^2 = M_A^2 + M_{lf}^2 - 2M_A E_{lf}^C . \tag{G7}$$

Here, E_{lf}^C is the final lepton's energy in the cm frame. From now on, all the quantities in the cm will be labeled in this way. So, for given E_{li}^L , i.e., M_A , we can see that

$$M_n + M_\pi \leq M_{\pi n} \leq M_A - M_{lf} . \tag{G8}$$

By using Eq. (G7), we find

$$(E_{lf}^C)_{\max} = \frac{M_A^2 + M_{lf}^2 - (M_{\pi n}^2)_{\min}}{2M_A}, \quad (\text{G9})$$

$$(E_{lf}^C)_{\min} = \frac{M_A^2 + M_{lf}^2 - (M_{\pi n}^2)_{\max}}{2M_A}. \quad (\text{G10})$$

Then, for given E_{li}^L and $M_{\pi n}$ (or E_{lf}^C), using $Q^2 = -M_{lf}^2 + 2E_{li}^C E_{lf}^C - 2E_{li}^C |\vec{p}_{lf}|^C \cos \theta_{lf}^C$ (where θ_{lf}^C is the angle between the outgoing lepton's direction and the incoming lepton's direction in the cm frame, and $E_{li}^C = (M_A^2 - M_n^2)/2M_A$ is the initial lepton's energy in the cm frame), we finally arrive at

$$[Q^2(E_{lf}^C)]_{\min} = -M_{lf}^2 + \frac{2E_{li}^C M_{lf}^2}{E_{lf}^C + \sqrt{(E_{lf}^C)^2 - M_{lf}^2}}, \quad (\text{G11})$$

$$[Q^2(E_{lf}^C)]_{\max} = -M_{lf}^2 + 2E_{li}^C \left(E_{lf}^C + \sqrt{(E_{lf}^C)^2 - M_{lf}^2} \right). \quad (\text{G12})$$

These equations give a description of the phase-space boundary in terms of the invariants $M_{\pi n}$ and Q^2 .

-
- [1] A. A. Aquilar-Arevalo *et al.* [MiniBooNE Collaboration], Phys. Rev. Lett. **100**, 032301 (2008) [arXiv:hep-ex/0706.0926].
 - [2] S. Nakayama *et al.* [K2K Collaboration], Phys. Lett. B **619**, 255 (2005).
 - [3] B. D. Serot and J. D. Walecka, Adv. Nucl. Phys. **16**, 1 (1986).
 - [4] B. D. Serot and J. D. Walecka, Int. J. Mod. Phys. E **6**, 515 (1997).
 - [5] R. J. Furnstahl, B. D. Serot, and H.-B. Tang, Nucl. Phys. **A615**, 441 (1997); **A640**, 505 (1998) (E).
 - [6] R. J. Furnstahl and B. D. Serot, Nucl. Phys. **A671**, 447 (2000).
 - [7] R. J. Furnstahl and B. D. Serot, Nucl. Phys. **A673**, 298 (2000).
 - [8] R. J. Furnstahl and B. D. Serot, Comments Mod. Phys. **2**, A23 (2000).
 - [9] B. D. Serot, Lecture Notes in Physics **641**, G. A. Lalazissis, P. Ring, and D. Vretenar, eds. (Springer, Berlin Heidelberg, 2004), p. 31.
 - [10] B. D. Serot, Ann. of Phys. **322**, 2811 (2007).
 - [11] M. A. Huertas, Phys. Rev. C **66**, 024318 (2002); **67**, 019901 (2003) (E).
 - [12] M. A. Huertas, Acta Phys. Polon. B **34**, 4269 (2003).
 - [13] M. A. Huertas, Acta Phys. Polon. B **35**, 837 (2004).
 - [14] J. McIntire, Acta Phys. Polon. B **35**, 2261 (2004).
 - [15] J. McIntire, arXiv:nucl-th/0507006.
 - [16] J. D. Walecka, Theoretical Nuclear and Subnuclear Physics, second ed. (World Scientific, Singapore, 2004), ch. 24.
 - [17] J. McIntire, Y. Hu, and B. D. Serot, Nucl. Phys. **A794**, 166 (2007).
 - [18] Y. Hu, J. McIntire, and B. D. Serot, Nucl. Phys. **A794**, 187 (2007).
 - [19] J. McIntire, Ann. of Phys. **323**, 1460 (2008).

- [20] B. D. Serot, Phys. Rev. C **81**, 034305 (2010) [arXiv:0912.5109 (nucl-th)].
- [21] J. Gasser and H. Leutwyler, Ann. Phys. (NY) **158**, 142 (1984).
- [22] S. L. Adler, Ann. Phys. (NY) **50**, 189 (1968).
- [23] C. H. Llewellyn-Smith, Phys. Rep. **3**, 261 (1972).
- [24] P. A. Schreiner and F. Von Hippel, Phys. Rev. Lett. **30**, 339 (1973).
- [25] D. Rein and L. M. Sehgal, Ann. Phys. (NY) **133**, 79 (1981).
- [26] L. Alvarez-Ruso, S. K. Singh, and M. J. Vicente Vacas, Phys. Rev. C **59**, 3386 (1999).
- [27] T. Sato, D. Uno, and T. S. H. Lee, Phys. Rev. C **67**, 065201 (2003).
- [28] O. Lalakulich and E. A. Paschos, Phys. Rev. D **71**, 074003 (2005).
- [29] O. Lalakulich, E. A. Paschos, and G. Piranishvili, Phys. Rev. D **74**, 014009 (2006).
- [30] E. Hernández, J. Nieves, and M. Valverde, Phys. Rev. D **76**, 033005 (2007).
- [31] K. M. Graczyk and J. T. Sobczyk, Phys. Rev. D **77**, 053001 (2008).
- [32] K. M. Graczyk, D. Kiełzewska, P. Przewłocki, and J. T. Sobczyk, Phys. Rev. D **80**, 093001 (2009).
- [33] O. Lalakulich, T. Leitner, O. Buss, and U. Mosel, Phys. Rev. D **82**, 093001 (2010) [arXiv:1007.0925 (hep-ph)].
- [34] G. M. Radecky *et al.*, Phys. Rev. D **25**, 1161 (1982).
- [35] T. Kitagaki *et al.*, Phys. Rev. D **34**, 2554 (1986).
- [36] C. Praet, O. Lalakulich, N. Jachowicz, and J. Ryckebusch, Phys. Rev. C **79**, 044603 (2009).
- [37] S. Weinberg, Phys. Rev. **166**, 1568 (1968).
- [38] S. Coleman, J. Wess, and B. Zumino, Phys. Rev. **177**, 2239 (1969).
- [39] C. G. Callan, Jr., S. Coleman, J. Wess, and B. Zumino, Phys. Rev. **177**, 2247 (1969).
- [40] S. Weinberg, Physica **96A**, 327 (1979).
- [41] J. Gasser and H. Leutwyler, Nucl. Phys. **B250**, 465 (1985).
- [42] S. Scherer, Adv. Nucl. Phys. **27**, 277 (2003).
- [43] H. Georgi and A. Manohar, Nucl. Phys. **B234**, 189 (1984).
- [44] H. Georgi, Phys. Lett. B **298**, 187 (1993).
- [45] P. J. Ellis and H.-B. Tang, Phys. Rev. C **57**, 3356 (1998).
- [46] R. J. Furnstahl, H.-B. Tang, and B. D. Serot, Phys. Rev. C **52**, 1368 (1995).
- [47] R. J. Furnstahl, B. D. Serot, and H.-B. Tang, Nucl. Phys. **A598**, 539 (1996).
- [48] C. Itzykson and J.-B. Zuber, Quantum Field Theory (McGraw–Hill, New York, 1980), ch. 12.
- [49] J. F. Donoghue, E. Golowich, and B. Holstein, Dynamics of the Standard Model (Cambridge, New York, 1992), ch. 2.
- [50] X. Zhang, Ph.D. thesis, Indiana University, 2011.
- [51] S. M. Ananyan, B. D. Serot, and J. D. Walecka, Phys. Rev. C **66**, 055502 (2002).
- [52] J. J. Kelly, Phys. Rev. C **70**, 068202 (2004).
- [53] T. Ericson and W. Weise, Pions and Nuclei (Clarendon Press, Oxford, 1988).
- [54] W. Rarita and J. Schwinger, Phys. Rev. **60**, 61 (1941).
- [55] K. Johnson and E. C. G. Sudarshan, Ann. Phys. (NY) **13**, 126 (1961).
- [56] C. R. Hagen, Phys. Rev. D **4**, 2204 (1971).
- [57] A. Z. Capri and R. L. Kobes, Phys. Rev. D **22**, 1967 (1980).
- [58] G. Velo and D. Zwanziger, Phys. Rev. **186**, 1337 (1969).
- [59] L. P. S. Singh, Phys. Rev. D **7**, 1256 (1973).
- [60] V. Pascalutsa, Phys. Rev. D **58**, 096002 (1998).
- [61] V. Pascalutsa, Phys. Lett. B **503**, 85 (2001).
- [62] H. Krebs, E. Epelbaum, and Ulf-G. Meißner, Phys. Rev. C **80**, 028201 (2009).

- [63] H.-B. Tang and P. J. Ellis, Phys. Lett. B **387**, 9 (1996).
- [64] H. Krebs, E. Epelbaum, and Ulf-G. Meißner, Phys. Lett. B **683**, 222 (2010).
- [65] C. Amsler *et al.* [Particle Data Group], Phys. Lett. B **667**, 1 (2008).
- [66] V. Pascalutsa, Prog. Part. Nucl. Phys. **61**, 27 (2008).
- [67] R. J. Hill, Phys. Rev. D **81**, 013008 (2010) [arXiv:0905.0291v1 (2009)].
- [68] P. J. Ellis and H.-B. Tang, Phys. Rev. C **56**, 3363 (1997).
- [69] S. Weinberg, The Quantum Theory of Fields, vol. I: Foundations (Cambridge, New York, 1995), sec. 5.3.
- [70] P. Van Nieuwenhuizen, Phys. Rep. **68**, 189 (1981).
- [71] M. Benmerrouche, R. M. Davidson, and N. C. Mukhopadhyay, Phys. Rev. C **39**, 2339 (1989).